学位論文（博士）

Role of the brain reward network in pain modulation

2018 年 3 月

星薬科大学大学院　薬学研究科
総合薬科学専攻
薬理学

渡邉　萌

Table of Contents

Abbreviations

AA: Amino acid

AAV: Adeno-associated virus

AAV6: Adeno-associated virus serotype 6

aCSF: artificial Cerebrospinal fluid

ANOVA: Analysis of variance

AP: Anteroposterior

ATP: Adenosine triphosphate

ChR2: Channelrhodopsin-2

CP: Caudoputamen

CW: Continuous-wave

DA-d_4: Deuterium labeled dopamine

DAT: Dopamine transporter

DiI: 1,1'-Dioctadecyl-3,3,3',3'-tetramethyl indocarbocyanine perchlorate

DPP: 2,4-Diphenyl-pyranylium

DRG: Dorsal root ganglion

DV: Dorsoventral

EGFP: Enhanced green fluorescent protein

EGTA: Ethylene glycol tetraacetic acid

ES: External standard

FLEX: Flip-excision

GABA: Gamma-aminobutyric acid

GCP-II: Glutamate carboxypeptidase II

GTP: Guanosine triphosphate

HRMS: high-resolution mass spectrometry

IC: Ion chromatography

IC-HRMS: Ion chromatography coupled with high-resolution mass spectrometry

IMDM: Iscove's modified Dulbecco's medium

IMS: Imaging mass spectrometry

IS: Internal standard

MALDI: Matrix assisted laser desorption ionization

MES: 2-Morpholinoethanesulfonic acid

mGluR: Metabotropic glutamate receptor

ML: Mediolateral

MOR: μ-opioid receptor

MS: Mass spectrometry

MSNs: Medium spiny neurons

NAA: N-Acetylaspartate

NAAG: N-Acetylaspartylglutamate

N.Acc.: Nucleus accumbens

NSAIDs: Non-steroidal anti-inflammatory drugs

PBS: Phosphate buffered saline

PFA: Paraformaldehyde

PL: Prelimbic cortex

PMPA: 2-(Phosphonomethyl)pentanedioic acid

QOL: Quality of life

SNL: Sciatic nerve ligation

VTA: Ventral tegmental area

Structures of drugs used in the present study

Morphine: [(5α, 6α)-7,8-didehydro-4, 5-epoxy-17-methylmorphinan-3,6-diol]

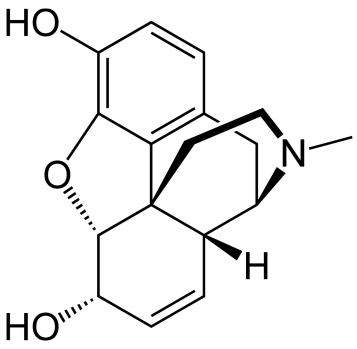

NAAG (N-acetylaspartylglutamate)

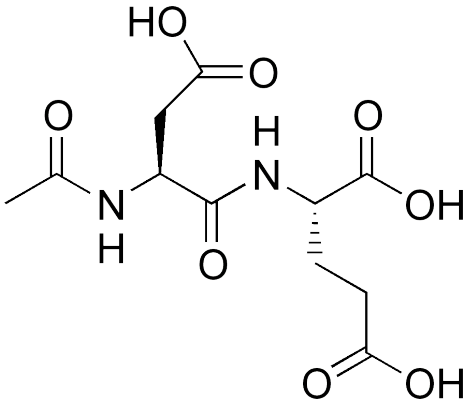

PMPA [2-(phosphonomethyl) pentanedioic acid]

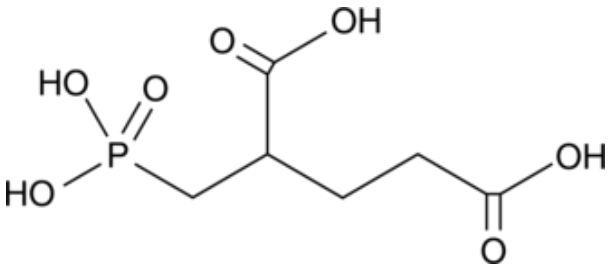

General Introduction

Neuropathic pain

Neuropathic pain, which is initiated or caused by a primary lesion or dysfunction in the nervous system, induces hypersensitivity to both noxious stimuli (hyperalgesia) and non-noxious stimuli (allodynia). Patients with neuropathic pain frequently have difficulty sleeping, and thereby, sleep deprivation produces depression and anxiety, which make the pain worse, leading to a vicious downward spiral. Since general analgesics such as non-steroidal anti-inflammatory drugs (NSAIDs) and opioids are often unable to control neuropathic pain, more effective measures for the management of neuropathic pain are required.

Cancer pain

The most common and severe pain in patients with advanced cancer is the pain associated with bone cancer. Various types of cancer metastasize to skeletal bones and cause spontaneous bone pain and hyperalgesia. Tumor growth in bone can induce pain by directly injuring nerve fibers that innervate the bone[1)]. Since cancer patients now live longer due to advances in cancer treatment, they also must face the challenge of severe and chronic tumor-induced pain, which is one of the most difficult chronic

pains to fully control. Cancer pain is a primary determinant of the patient's quality of life, and thus effective pain control is required.

Mesolimbic dopaminergic neurons

Mesolimbic dopaminergic neurons originate in the ventral tegmental area (VTA) and mainly project to the nucleus accumbens (N.Acc.). These neurons are well recognized to play important roles in positive and negative reinforcement, approach behavior, decision-making, working memory, stimulus salience, incentive salience and the expression of positive emotions such as pleasure and happiness[2-8]. Mesolimbic dopaminergic neurons display two distinct tonic and phasic firing patterns. Tonic firing refers to slow and irregular firing, while phasic firing refers to a rapid series of action potentials occurring with a short inter-spike interval (burst firing)[9]. In particular, phasic firing is observed following unpredicted or better-than-expected rewards[10,11].

Optogenetics

Optogenetics is a relatively new method in neuroscience that has been developed in over the last decade. Dr. Karl Deisseroth, who pioneered this method, defined it as "the combination of genetic and optical methods to achieve gain or loss of function of well-defined events in specific cells of living tissue"[12-14]. To control the activity of

targeted cells with spatiotemporal precision through the use of light, a technique to specifically express light-sensitive opsins, which can directly elicit electrical current across cellular membranes in response to light, in the targeted cells is required. In general, virus vectors and/or transgenic animals that have well-engineered properties (e.g., axonal and/or retrograde transduction, cell type-specific promoter dependence and/or recombinase dependence) are used for the anatomical and cell type-specific expression of opsin.

In vivo Cre-loxP approach

The Cre-loxP system has been widely used to achieve cell-specific gene expression. In this system, an enzyme that was originally derived from the P1 bacteriophage, Cre recombinase, recognizes the *loxP* site, a specific DNA sequence of 34 base pairs, and catalyzes recombination between two *loxP* sites[15,16]. The genetic materials will be rearranged (inversion, deletion and translocation) depending on the relative location and orientation of the two *loxP* sites. For cell-type-specific expression of a targeted gene *in vivo*, various types of virus and/or transgenic animals carrying Cre or loxP are used. The flip-excision (FLEX) switch system is frequently used for cell- specific gene expression[17]. This system involves two recombination steps: an inversion followed by an excision. First, Cre recombinase binds to *loxP* sites and flips the gene located between two pairs of heterotypic antiparallel *loxP* sites through recombination

between either pair of homotypic sites. Two homotypic *loxP* sites are then positioned in a direct orientation, resulting in excisional recombination. The final product has an inverted gene flanked by two heterotypic *loxP* sites that cannot recombine with each other, which prevents further inversions.

Optogenetic approach to induce acute pain

The optogenetic approach using adeno-associated virus (AAV) serotype 6 developed by Iyer et al.[18] is useful for inducing pain-related behavior in freely moving mice at high temporal resolution. AAV serotype 6 (AAV6) has been used for retrograde gene delivery in the periphery and brain[19,20]. In particular, it has previously been reported to specifically transduce nociceptive neurons by intrasciatic injection[21]. Thus, injection of engineered AAV6 carrying the blue light-activated nonselective cation channel channelrhodpsin-2 (ChR2) gene into the sciatic nerve enables specific expression of ChR2 in the nociceptive neurons innervating the hind paw. Furthermore, blue light illumination of the plantar surface of the ipsilateral hind paw induces pain-related behavior and reduces mechanical thresholds, consistent with the activation of nociceptors.

Mass spectrometry

Mass spectrometry (MS) is becoming increasingly important as an analytical technique in bioscience research. Using this technique, researchers can detect, identify and quantitate known or unknown molecules based on their mass-to-charge (m/z) ratio. Mass spectrometer consists of several components, including an inlet system, an ion source, a mass analyzer and a detector. To enhance the mass-resolving and -determining capabilities of mass spectrometry, chromatographic and other separation techniques (e.g., gas chromatography, liquid chromatography, ion chromatography, capillary electrophoresis, etc.) are used in the inlet system. Separated samples are ionized by various methods, and then analyzed according to their mass-to-charge ratio through mass analyzers. The important parameters of a mass analyzer are its mass-resolving power and mass range. The various methods available for use, including Magnetic Sector, Quadrupole, Ion Trap, Time-of-Flight, Fourier-Transform Ion Cyclotron Resonance or Accelerator Mass Spectrometry, should be selected depending on the required property for analysis. Separated ions are recorded as a current when they hit the surface of a detector, and mass spectra are then generated.

Imaging mass spectrometry

Imaging mass spectrometry (IMS) is an effective technique for obtaining a combination of molecular information and good spatial resolution in cells and tissue sections[22,23]. It enables the visualization of the distribution of small molecules, including both exogenous drugs and endogenous metabolic intermediates such as lipids, amino acids, and organic acids[24-26]. Because of the MS-based detection principle, IMS offers several advantages: i) it does not require any labels or specific probes to detect molecules, ii) it is non-targeted and thus can be used to obtain information about unexpected molecules, and iii) it allows simultaneous visualization of the tissue distributions of various types of molecules.

Co-existence and its heterogeneity of neurotransmitters in neurons

Neurotransmitters are endogenous small molecules released from presynaptic nerve terminals. They act as chemical messengers that are used by neurons to communicate with each other and with other types of cells by binding to specific receptors on postsynaptic cells. There are several criteria for identifying neurotransmitters: (i) they are stored in vesicles in presynaptic nerve terminals, (ii) they are synthesized by and released from presynaptic neurons in response to membrane depolarization, (iii) they produce specific responses at postsynaptic cells by binding to specific receptors, and (iv) they are inactivated by reuptake into presynaptic neurons or glia, or are

metabolized by enzymes[27,28]. Furthermore, they can be classified as classical neurotransmitters or neuropeptides including small molecules. Classical neurotransmitters include choline (acetylcholine), monoamines (dopamine, noradrenaline, serotonin, etc.), amino acids (gamma-aminobutyric acid (GABA), glutamate, etc.) and purines (adenosine, adenosine triphosphate, etc.). On the other hand, neuropeptides include opioid peptides (pro-enkephalin, pro-opiomelanocortin, pro-dynorphin, etc.), hypothalamic releasing factors (corticotrophin-releasing hormone, growth hormone-releasing hormone, somatostatin, etc.), pituitary hormones (adrenocorticotropic hormone, α-melanocyte-stimulating hormone, prolactin, etc.), neurohypophyseal peptides (oxytocin, vasopressin), neuronal and endocrine peptides (calcitonin gene-related peptide, vasoactive intestinal peptide, etc.), circulating peptides (angiotensin, bradykinin), gastrointestinal and brain peptides (cholecystokinin, neurotensin, substance P, etc.) and gastrointestinal and pancreatic peptides (glucagon, etc.). Many neurons can release multiple neurotransmitters, not just one. Recently, the physiological role of the co-release of multiple transmitters has been revealed incrementally.

N-Acetylaspartylglutamate

N-Acetylaspartylglutamate (NAAG) is a neuropeptide that was discovered in the mammalian brain in the mid-1960s. It met the criteria to be accepted as a

neurotransmitter between 1985 and 2000[29,30]. NAAG is synthesized from N-acetylaspartate (NAA) and glutamate[31-33] by NAAG synthetase I and NAAG synthetase II[34,35]. After it is released from presynaptic terminals, NAAG is considered to activate Group II metabotropic glutamate receptors (mGluR), particularly mGluR3[36]. Although the activation of presynaptic mGluR3 by NAAG could inhibit the synaptic release of neurotransmitters, the effects of NAAG on postsynaptic mGluR3 have not been completely explained, except for the reduction of cyclic adenosine monophosphate (cAMP) levels via an inhibitory G proteins[37,38].

Aim and Scope

The aim of the present study was to investigate the role of the mesolimbic dopaminergic system in pain modulation. To achieve this goal, behavioral biochemical and molecular biological experiments were performed.

The specific aims of the proposed research are as follow:

In Chapter 1:

To clarify the influence of chronic pain on mesolimbic dopaminergic neurons, I measured the excitability of mesolimbic dopaminergic neurons under conditions of neuropathic or cancer pain using electrophysiology.

In Chapter 2:

To ascertain the role of the activity of mesolimbic dopaminergic neurons in pain modulation, I examined whether the activation of mesolimbic dopaminergic neurons could alleviate nerve injury- or tumor-induced allodynia using optogenetic methods.

In Chapter 3:

To identify potential pain modulators released in the N.Acc., I simultaneously analyzed the small molecules in brain fluids using a combined microdialysis/mass spectrometry system, under both the application of pain stimuli and the administration of analgesics.

Ethics

The present study was conducted in accordance with the Guiding Principles for the Care and Use of Laboratory Animals, Hoshi University, as adopted by the Committee on Animal Research of Hoshi University, which is accredited by the Ministry of Education, Culture, Sports, Science, and Technology of Japan. Every effort was made to minimize the numbers and any suffering of animals used in the following experiments. Animals were used only once in the present study.

Chapter 1

Effect of chronic pain on the brain reward network

Introduction

Pain can elicit negative emotional state[39] and diminish quality of life (QOL), which have been recognized as important parameters for evaluating the effectiveness of medical therapies[40]. Thus, the improvement of patient QOL is one of the purposes for pain control.

The mesolimbic dopaminergic pathway is one of the neural systems that have been suggested to modulate positive or negative emotion[41]. Furthermore, substantial evidence has implicated the mesolimbic dopaminergic reward valuation pathway in both acute and chronic pain states. Particularly, chronic pain is accompanied by adaptive changes within central circuits that amplify the consequences of sensory inputs. On the other hand, neuropathic pain results from damage or dysfunction of nerves and is chronic, debilitating, and is often characterized by ongoing pain as well as hyperalgesia and allodynia. Bone cancer pain has been suggested to result from the contributions of structural, inflammatory and neuropathic components that promote ongoing pain, breakthrough pain and hypersensitivity to normally innocuous stimuli. However, not enough is known about the effects of these chronic pain states in the mesolimbic reward network.

In the present study, I hypothesized that neuropathic or bone cancer pain would produce pronociceptive adaptive changes in mesolimbic dopaminergic neurons. I used electrophysiological techniques to investigate the excitability of mesolimbic dopaminergic neurons in mice with neuropathic or cancer pain.

Materials and methods

Animals

Male C57BL/6J mice (8-12 weeks old) (Tokyo Laboratory Animals Science Co., Ltd., Tokyo, Japan) were used in this study. All mice were housed up to 6 mice per cage and kept in a temperature- and humidity-controlled room (24 ± 1°C, 55 ± 5% relative humidity) under a 12 hr light-dark cycle (light on at 8 a.m.). Food and water were available *ad libitum*. Behavioral tests were performed in the light phase. Mice were randomly selected for inclusion in each group by cage prior to baseline testing.

Neuropathic pain model

Mice were deeply anesthetized with isoflurane (3%, inhalation). I produced a partial nerve ligation model by using an 8-0 silk suture tightly ligated around approximately one-half of the diameter of the sciatic nerve in the right (ipsilateral) hind paw, as previously described[42, 43]. In sham-operated mice, the nerve was exposed but not ligated.

Thermal paw withdrawal test

A thermal stimulus generated using a thermal stimulus apparatus (Model 7360; UGO BASILE, Varese, Italy; model 33 Analgesia Meter; IITC/Life Science Instruments, CA, USA)

was applied to the plantar surface of the mouse's hind paw to assess thermal paw-withdrawal thresholds. The intensity of the thermal stimulus was adjusted to achieve an average baseline paw-withdrawal latency of approximately 8 to 10 sec in naive mice. A cut-off time of 15 sec was used to prevent tissue damage. Quick hind paw movements away from the stimulus were considered to be a withdrawal response.

Electrophysiology

1,1'-Dioctadecyl-3,3,3',3'-tetramethyl indocarbocyanine perchlorate (DiI; 0.75 μL of 1%; Molecular Probes, OR, USA) was stereotactically infused into the N.Acc. (from bregma: anteroposterior (AP) +1.6 mm, mediolateral (ML) +1.8 mm, dorsoventral (DV) -4.0 mm at an angle of 10°) of sciatic nerve-ligated mice at a rate of 0.25 μL/min. One week after the operation, mice were anesthetized and perfused transcardially with ice-cold sucrose artificial cerebrospinal fluid (aCSF), which contained (in mM) 222.1 sucrose, 2.5 KCl, 1.4 NaH_2PO_4, 1 $CaCl_2$, 7 $MgCl_2$, 27 $NaHCO_3$ and 0.5 ascorbic acid (oxygenated with 95% O_2 and 5% CO_2). Coronal brain slices (300 μm thick) containing the VTA re prepared with a vibratome (VT 1200S; Leica, tzlar, Germany) in cold sucrose-aCSF. The slices were kept at room temperature for at least 1 hr before recording in an oxygenated standard aCSF that contained (in mM) 128 NaCl, 3 KCl, 1.25 NaH_2PO_4, 2 $CaCl_2$, 2 $MgCl_2$, 24 $NaHCO_3$ and 10 glucose.

Whole-cell current-clamp recordings were made only from fluorescently DiI-labeled VTA neurons that were visually identified by using an upright microscope (Eclipse FN1; Nikon,

Tokyo, Japan) equipped with G2-A filters. Slices were superfused at ~2 ml/min with standard aCSF at 30-32 °C. Patch pipettes (4-6 MΩ) re pulled from borosilicate glass (Harvard App., GC150-7.5) on a pipette puller (P-97; Sutter Instruments, CA, USA) and filled with internal solution (pH 7.25 with KOH) consisting of (in mM) 120 K-gluconate, 10 KCl, 10 creatine phosphate, 4 Mg-adenosine triphosphate (ATP), 0.3 Na_2-guanosine triphosphate (GTP), 0.2 ethylene glycol tetraacetic acid (EGTA) and 0.2% biocytin. Signals were obtained using a Multiclamp 700B amplifier (Molecular Devices, CA, USA), filtered at 2 kHz, digitized at 10 kHz using a Digidata 1544 analog-to-digital converter (Molecular Devices) and stored using pClamp software (Molecular Devices). To probe intrinsic neuronal excitability, VTA neurons were injected with a 2-s current pulse at 50 pA increments ranging from 0-200 pA. The number of action potentials evoked by each current step was quantified. Action potential amplitudes were measured from the resting membrane potential, and action potential half-widths were measured at 50 % of the peak. The threshold for action potential initiation was defined as the beginning of the upstroke of the spike. The amplitudes of afterhyperpolarizations were measured from the spike threshold to its peak. Resting membrane potentials were measured immediately after patch rupture and were not corrected for liquid junction potential. Series resistance (15-25 M) and input resistance re monitored throughout each experiment.

Immunostaining after electrophysiology

Following electrophysiological recordings, slices were immediately fixed in 4% paraformaldehyde (PFA) in phosphate buffered saline (PBS). The sections were incubated in appropriate blocking solution and then incubated with mouse monoclonal tyrosine hydroxylase antibody (1:4500, Immunostar, WI, USA). After washes, the samples were treated with Alexa Fluor 488 goat anti-mouse antibody (1:5000, Thermo Fisher Scientific, Inc., MA, USA) or streptavidin conjugated with Alexa 647 (1:3000, Thermo Fisher Scientific, Inc.). The sections were mounted with ProLong Diamond Antifade Mountant with DAPI (Thermo Fisher Scientific, Inc.). Fluorescence of immunolabeling was detected using an All-in-One microscope (BZ-X710, Keyence, Osaka, Japan).

Cell culture

Mouse osteosarcoma AXT cells were established as previously described[44] and were cultured under 5% CO_2 at 37°C in Iscove's modified Dulbecco's medium (IMDM) (Thermo Fischer Scientific, CA, USA) supplemented with 10% fetal bovine serum.

Tumor xenograft model

To establish tumor xenografts, AXT cells (1×10^6) suspended in 50 ml of IMDM were injected into the right femoral bone marrow cavity of syngeneic C57BL/6J mice. Briefly, the knee joint was flexed to 90° and the distal side of the femur was exposed by incising the skin.

A 23-gauge needle was inserted into the bone marrow cavity to make a small hole, into which AXT cells or medium alone were injected. All procedures were performed under inhalational anesthesia with 3% isoflurane.

Statistical analysis

The data are presented as the mean ± S.E.M. I chose the sample size based on similar publications in the field. The statistical significance of differences between the groups was assessed by two-way analysis of variance (ANOVA) followed by the Bonferroni multiple comparisons test or Sidak's test. All statistical analyses weßre performed with GraphPad Prism 5.0 (GraphPad Software, CA, USA). A p value of < 0.05 was considered to reflect significance.

Results

Decreased excitability of mesolimbic dopamine neurons under neuropathic pain

Sciatic nerve ligation (SNL) as a model of neuropathic pain resulted in a marked decrease in the latency of ipsilateral hind paw withdrawal in response to normally non-noxious heat (i.e., thermal allodynia) (Figure 1-1a). In the previous studies, it was hypothesized that nerve injury may affect the activity of the VTA-opioid-dopamine network[45]. However, it remained unclear whether severe pain including cancer pain could negatively control the neuronal activity of the mesolimbic reward network and whether specific activation of this pathway could reverse hyperalgesia and allodynia related to neuropathic and cancer pain.

VTA dopamine neurons project to the N.Acc., prefrontal cortex, hippocampus, basolateral amygdala and other regions that participate in the modulation of pain[46-48]. To label VTA neurons terminating in the N.Acc., I injected DiI, a retrograde red fluorescent tracer, into the N.Acc. on the side contralateral to the SNL (Figures 1-1b to d). I performed patch-clamp electrophysiology for DiI-labeled neurons in the VTA to characterize the impact of SNL on dopaminergic neurons projecting to the N.Acc. The DiI-positive neurons in the VTA were characterized as dopaminergic nerves by co-labeling for the enzyme tyrosine hydroxylase (Figure 1-1e). I used patch-clamp electrophysiology in VTA slices from SNL- and sham-operated mice to investigate the intrinsic neuronal excitability of DiI-labeled neurons. In response to current injection, the number of spikes in DiI-positive

and TH-positive neurons was significantly lower in the SNL group than in the sham group at all levels of current tested (Figure 1-1f and g). There were no significant differences in other electrophysiological properties of VTA dopamine neurons between the two groups (Table 1).

Decreased excitability of mesolimbic dopamine neurons under cancer pain

To produce a tumor-induced bone pain model, used severe osteosarcoma cells (AXT cells). AXT cells re established *in vitro* from an AX cell-derived subcutaneous osteosarcoma, which was obtained by overexpression of *c-MYC* in bone marrow stromal cells derived from Ink4a/Arf (-/-) mice (Figure 1-2a). The intrafemoral bone marrow injection of AXT cells (Figure 1-2b) resulted in a marked decrease in the ipsilateral hind paw-withdrawal latency induced by normally non-noxious heat (Figure 1-2c). To label VTA neurons terminating in the N.Acc., I injected DiI into the N.Acc. on the side contralateral to the intrafemoral bone marrow implantation of osteosarcoma cells (Figures 1-2d to f). After confirming that DiI-positive neurons in the VTA were dopaminergic by co-labeling for TH (Figure 1-2g), I used patch-clamp electrophysiology in VTA slices from tumor-bearing mice to investigate the intrinsic neuronal excitability of DiI-labeled neurons. As a result, the number of spikes in DiI-positive and TH-positive neurons was significantly lower in the tumor-bearing group than in the control group at all levels of current tested (Figure 1-2h and i). There were no

significant differences in other electrophysiological properties of VTA dopamine neurons between the two groups (Table 2).

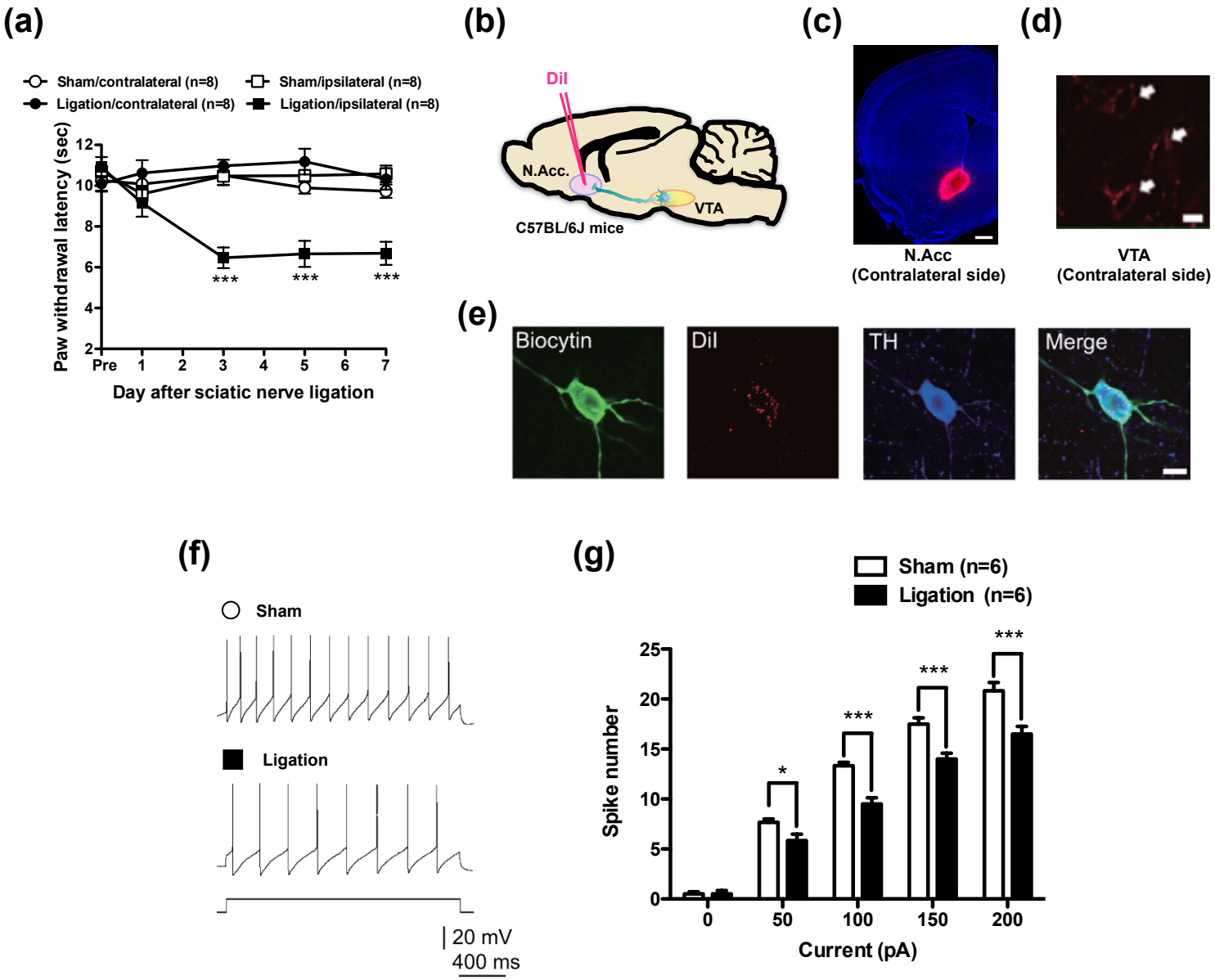

Figure 1-1

Sciatic nerve ligation decreases the excitability of mesolimbic dopaminergic neurons

(a) Latency of paw withdrawal in response to thermal stimulation after sham (n = 8) or sciatic nerve ligation (n = 8) (Sham-contralateral vs Sham-ipsilateral, $F_{4,56}$ = 1.12; Sham-contralateral vs Ligation-ipsilateral, $F_{4,56}$ = 0.76; Ligation-contralateral vs Ligation-ipsilateral, $F_{4,56}$ = 11.13; Sham-ipsilateral vs Ligation-ipsilateral, $F_{4,56}$ = 9.98). (b) Schematic of the experimental design. (c) DiI retrograde tracer injection site. Scale bar = 500 μm. (d) DiI-labeled neurons in the VTA. Scale bar = 10 μm. (e) Confocal images of biocytin-stained DiI-positive and TH-positive neurons. Scale bar = 10 μm. (f, g) Representative sample traces (f) and quantification of action potentials in response to increasing current injections (g) (n = 6, $F_{4,20}$ = 9.428). Data are mean ± S.E.M. *p < 0.05; ***p < 0.001; by two-way repeated measures analysis of variance (ANOVA) with a Bonferroni post hoc analysis (a) or Sidak's post hoc analysis (g).

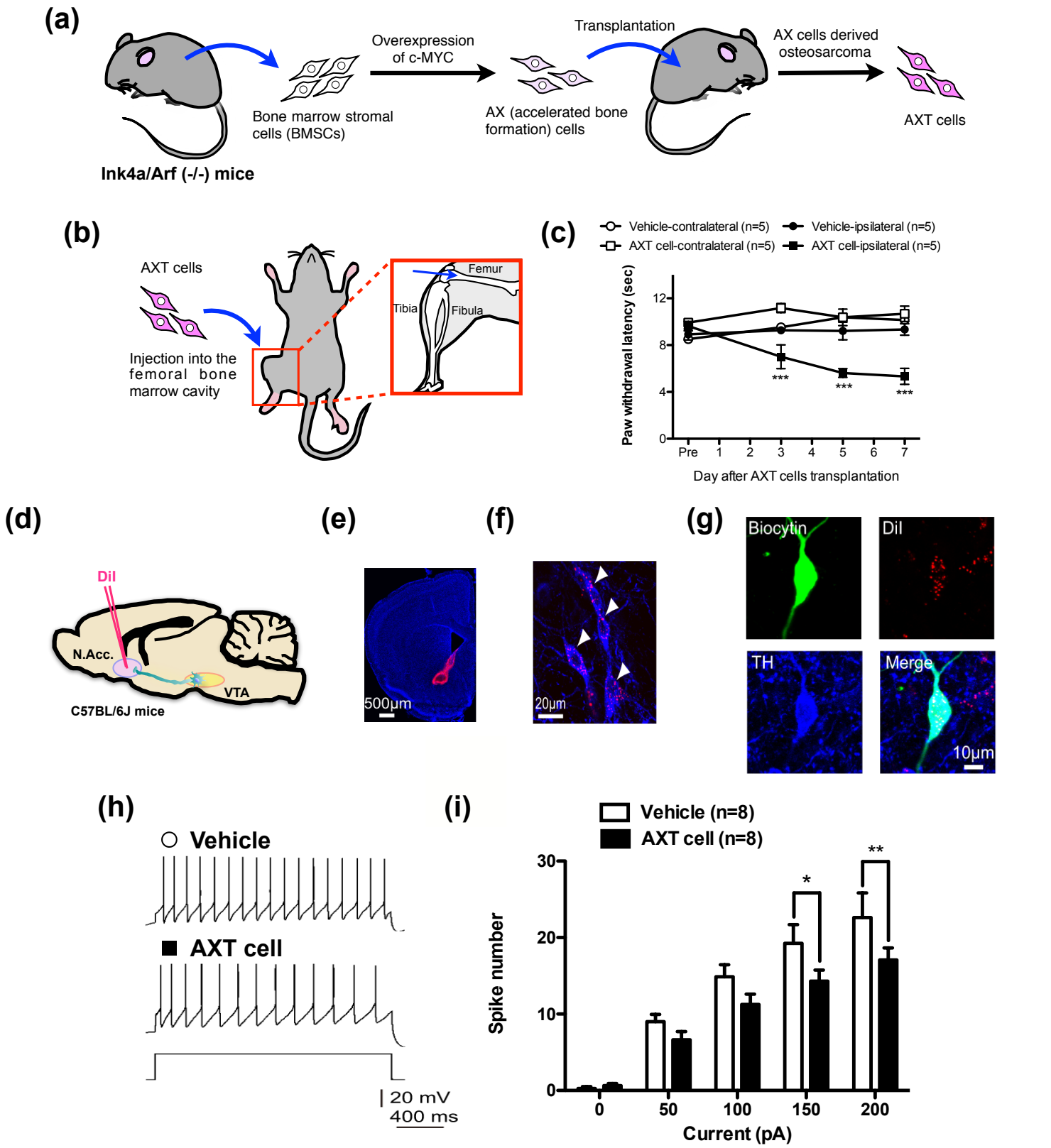

Figure 1-2

Cancer pain decreases the excitability of mesolimbic dopaminergic neurons.

(a, b) Schematic illustration of the establishment of AXT cells (Shimizu et al. 2010) (a) and injection site of AXT cells. (c) Latency of paw withdrawal in response to thermal stimulation after vehicle (n = 5) or AXT cell transplantation (n = 5) (Vehicle-contralateral vs Vehicle-ipsilateral, $F_{3,24} = 1.36$; Vehicle-ipsilateral vs AXT cell-ipsilateral, $F_{3,24} = 9.13$; AXT cell-contralateral vs AXT cell-ipsilateral, $F_{3,24} = 10.75$). (d) Schematic of the experimental design. (e) DiI retrograde tracer injection site. Scale bar = 500 μm. (f) DiI-labeled neurons in the VTA. Scale bar = 20 μm. (g) Confocal images of biocytin-stained DiI-positive and TH-positive neurons. Scale bar = 10 μm. (h, i) Representative sample traces (h) and quantification of action potentials in response to increasing current injections (i) (n = 8, $F_{4,28} = 2.223$). Data are mean ± S.E.M. *p < 0.05; **p < 0.01; ***p < 0.001; by two-way repeated measures ANOVA with a Bonferroni post hoc analysis (c) or Sidak's post hoc analysis (i).

Table 1: Electrophysiological properties of VTA dopamine neurons under neuropathic pain.

	Membrane potential (mV)	Spike threshold (mV)	Spike amplitude (mV)	Spike half-width (ms)	Spike AHP (mV)
Sham	-52.5±1.4	-36.4±1.2	-76.7±2.0	-1.09±0.07	25.9±0.9
Ligation	-55.0±0.9	-34.6±1.3	-80.3±2.5	-1.22±0.05	27.7±0.4

AHP, afterhyperpolarization.

Table 2: Electrophysiological properties of VTA dopamine neurons under cancer pain.

	Membrane potential (mV)	Spike threshold (mV)	Spike amplitude (mV)	Spike half-width (ms)	Spike AHP (mV)
Vehicle	-51.1±1.4	-32.5±1.2	-81.1±2.6	-1.25±0.05	27.6±1.7
AXT cells	-50.2±1.0	-30.9±1.0	-76.2±3.0	-1.37±0.12	25.8±2.3

AHP, afterhyperpolarization.

Discussion

Chronic pain has been suggested to be associated with a hypodopaminergic state[49-51], which is consistent with increased and decreased pain in patients with Parkinson's disease or schizophrenia, respectively[52-55]. Additionally, pain is often co-morbid with other psychiatric conditions including major depressive disorder that is characterized by anhedonia[56,57] and increased pain sensitivity[58]. Decreased tonic dopamine levels in the N.Acc. have been suggested to underlie a loss of inhibition of dopamine D_2 receptor-expressing indirect pathway output neurons that may promote hypersensitivity under pain[59] as well as increased impulsivity[60]. Ren et al. demonstrated a reduction in the spontaneous spiking of VTA dopaminergic neurons in VTA slices from mice with sciatic nerve ligation[50]. Here, I found that the firing of VTA dopamine neurons with confirmed projections to the N.Acc. was significantly decreased by sciatic nerve ligation and intrafemoral bone marrow injection of osteosarcoma cells, consistent with observations of decreased neural activity of VTA dopamine neurons and decreased dopaminergic activation of the N.Acc. in response to a noxious stimulus in patients with chronic pain[61,62]. It was previously proposed that the sustained release of β-endorphin in the VTA in the setting of sciatic nerve injury may lead to the down-regulation of VTA μ-opioid receptor function, resulting in the increased activity of GABAergic μ-opioid receptor (MOR)-expressing neurons and subsequently the inhibition of

mesolimbic dopamine neurons[63]. Indeed, based on the molecular tagging of cFos-expressing neurons, my preliminary data suggested that neuropathic pain increases the number of activated TH-negative (putative GABAergic) neurons (unpublished observation). Taken together, these findings suggested that sustained afferent input from nerve injury may result in the suppression of mesolimbic dopaminergic neurons through the activation of GABA neurons in VTA.

Chapter 2

Optogenetic activation of mesolimbic dopaminergic neurons alleviates neuropathic and cancer pain

Introduction

Circuits that mediate pain overlap, at least in part, with those associated with pleasure[64]. Thus, pain can be decreased by stimuli that promote positive emotions such as pleasant music, food or fragrances[65,66] while pain may reduce the motivation to seek natural rewards[67].

Patients with chronic pain suffer from a multitude of symptoms related to mechanisms of central amplification including ongoing (spontaneous) pain as well as allodynia and hyperalgesia[68]. The mechanistic underpinnings of these symptoms are likely to differ and are not well understood. Notably, however, painful responses to normally innocuous sensory signals promote learned avoidance behaviors that likely sustain pain chronicity[69]. These conditions are poorly managed with current therapies, which are largely ineffective in many patients. Both ongoing pain and allodynia are important clinical conditions that represent an important unmet medical need and are devastating the QOL of patients.

Opiates remain one of the most important classes of pain-relieving medicines. These drugs promote behavioral reinforcement and elicit a positive mood and euphoria through, in part, context-dependent phasic dopamine signals from dopamine neurons in the ventral tegmental area (VTA) that project to the nucleus accumbens (N.Acc.)[70] as well as the prefrontal and anterior cingulate cortices[71]. On the other hand, pain and pain relief are

salient stimuli that produce motivation for protective or escape behaviors that promote safety[72]. Furthermore, the relief of pain is rewarding and activates the VTA dopaminergic pathway[73]. However, the role of mesolimbic dopaminergic neurons in the modulation of allodynia and hyperalgesia remains unknown.

In the present study, I hypothesized that the activation of mesolimbic dopaminergic neurons would contribute to the modulation of nociception, particularly in pathological states. Here, I used neurochemical, optogenetic and behavioral techniques to demonstrate that increased dopamine release in the N.Acc. resulting from the activation of VTA dopaminergic neurons reverses evoked allodynia in mice with neuropathic or cancer pain without increasing threshold responses to physiological pain in sham-operated animals.

Materials and methods

Animals

Male C57BL/6J mice (8-12 weeks old) (Tokyo Laboratory Animals Science Co., Ltd., Tokyo, Japan) and TH-cre (B6.Cg-Tg (Th-cre) 1Tmd/J) mice (Jackson Laboratory, ME, USA) were used in this study. All mice were housed up to 6 mice per cage and kept in a temperature- and humidity-controlled room (24 ± 1°C, 55 ± 5% relative humidity) under a 12 hr light-dark cycle (light on at 8 a.m.). Food and water were available *ad libitum*. Behavioral tests were performed in the light phase. Mice were randomly selected for inclusion in each group by cage prior to baseline testing.

Neuropathic pain model

Partial sciatic nerve injury was conducted as previously described in Chapter 1.

Cell culture

Mouse osteosarcoma AXT cells were cultured as previously described in Chapter 1.

Tumor xenograft model

Tumor xenograft models were generated as previously described in Chapter 1.

Virus preparation

I purchased pAAV-Flex-rev-ChR2 (H134R)-mCherry (ID:18916) from Addgene (MA, USA). AAV-Flex-rev-ChR2 (H134R)-mCherry (AAV-Flex-ChR2) was serotyped with AAV5 coat proteins and packaged by the viral vector core at University of Kyoto (Drs. R. Matsui and D. Watanabe). The final viral concentration was 2×10^{13} particles/mL. These aliquots of virus were stored at -80°C until use.

Stereotaxic viral injection and cannula implantations

Stereotaxic injections were performed under isoflurane (3%) anesthesia and using small animal stereotaxic instruments (RWD Life Science, CA, USA). Virus (AAV-flex-ChR2) was bilaterally injected into the VTA (from bregma: AP -2.5 mm, AP ±1.3 mm, DV -4.8 mm at an angle of 10°), at a rate of 0.25 μL/min for 4 min. More than 2 weeks after virus injection, mice expressing light-sensitive protein were implanted with an 8 mm fiber cannula (EIM-330; Eicom, Kyoto, Japan) above the VTA (from bregma: AP -2.5 mm, ML ±1.3 mm, DV -3.8 mm at an angle of 10°) or N.Acc. (from bregma: AP +1.4 mm, ML ±1.5 mm, DV -3.1 mm at an angle of 10°). To combine optical stimulation with simultaneous microdialysis in the N.Acc., an optogenetics-compatible microdialysis probe (CX-F-6-01; Eicom) inserted into a guide cannula (CXGF-6; Eicom) was implanted above the N.Acc. (from bregma: AP +1.4 mm, ML +1.5 mm, DV -3.6 mm at an angle of 10°).

Optical stimulation

Optical fibers (250 μm diameter; Lucir, Ibaraki, Japan) were placed inside the fiber cannula. These fibers were connected to a 473 nm blue laser (COME2-LB473/100; Lucir), and light pulses were generated through an electronic stimulator (Nihon Kohden, Tokyo, Japan). Mice expressing ChR2 and their controls were illuminated by blue light (473 nm, 30 Hz, 5 ms, 8 pulses every 5 s) for 30 min.

Immunohistchemistry

Mice were deeply anesthetized with isoflurane (3%, inhalation) and transcardially perfusion-fixed with 4% PFA in 0.1 M phosphate-buffer (pH 7.4). Coronal brain sections were post-fixed and cryoprotected in 20-30 (w/v)% sucrose. Brain sections were then embedded in optimal cutting temperature compound (OCT compound; Tissue Tek; Sakura Fine Technical, Tokyo, Japan) and frozen sections were cut on a cryostat (CM1860 or CM1510; Leica Microsystems, Heidelberg, Germany) (8 μm). The brain sections were incubated in appropriate blocking solution and then incubated with mouse monoclonal anti-tylosine hydroxylase antibody (1:4500, Immunostar), rabbit polyclonal anti-mCherry antibody (1:1000, abcam plc., Cambridge, UK), rat monoclonal anti-DAT antibody (1:3500, Millipore, MA, USA). Following washes, they were incubated with Alexa Fluor 488 goat anti-mouse antibody (1:5000, Thermo Fisher Scientific), Alexa Fluor 488 goat anti-rat antibody (1:2000, Thermo Fisher Scientific), or Alexa Fluor 546 goat anti-rabbit antibody

(1:10000, Thermo Fisher Scientific). The sections were mounted with Dako fluorescent mounting medium (Dako, Glostrup, Denmark). Fluorescence of immunolabeling was detected using a light microscope (BX-61; Olympus, Tokyo, Japan) and photographed with a digital camera (CoolSNAP HQ; Olympus) or fluorescence microscope (BZ-X710; Keyence, Osaka, Japan).

In vivo microdialysis and high-performance liquid chromatography

A microdialysis probe was implanted directly into the N.Acc. (AP, +1.4 mm; AP, +1.5 mm; AP, -3.6 mm; angle, 10°). The probe was continuously perfused with artificial cerebrospinal fluid (0.9 mM $MgCl_2$, 147.0 mM NaCl, 4.0 mM KCl, and 1.2 mM $CaCl_2$) at a flow rate of 1 μL/min by a syringe pump (ESP-32; Eicom). Outflow fractions were collected every 15 min. After more than 2 baseline fractions were collected, mice were subjected to optical stimulation. Dialysis samples were analyzed by high-performance liquid chromatography with electrical detection (HTEC-500; Eicom). Dopamine was separated by column chromatography and identified according to the retention times of a dopamine standard. The amount of dopamine was quantified by calculations using the peak area and data are expressed as a % of the corresponding baseline peak area.

Thermal paw withdrawal test

A thermal stimulus generated using a thermal stimulus apparatus (Model 7360; UGO

BASILE, Varese, Italy) was applied to the plantar surface of the mouse's hind paw to assess thermal paw-withdrawal thresholds. The intensity of the thermal stimulus was adjusted to achieve an average baseline paw-withdrawal latency of approximately 8 to 10 sec in naive mice. A cut-off time of 15 sec was used to prevent tissue damage. Quick hind paw movements away from the stimulus were considered to be a withdrawal response.

Statistical analysis

The data are presented as the mean ± S.E.M. I chose the sample size based on similar publications in the field. The statistical significance of differences between the groups was assessed by one-way or two-way ANOVA followed by the Bonferroni multiple comparisons test. All statistical analyses were performed with GraphPad Prism 5.0 (GraphPad Software, La Jolla, CA). A p value of < 0.05 was considered to reflect significance.

Results

Activation of VTA dopamine neurons reversibly suppresses the allodynic effects of neuropathic pain

To investigate a causal link between VTA-dopamine neuron activity and thermal hyperalgesia following sciatic nerve ligation, we generated transgenic mice expressing a light-activated nonselective cation channel, channelrhodpsin-2 (ChR2), in VTA-dopamine neurons and specifically activated VTA-dopamine neurons. TH-cre mice were injected with AAV with the FLEX switch system to express ChR2 fused with mCherry (Figure 2-1a, AAV-CAG-Flex-rev-ChR2-mCherry) (TH-cre/ChR2 mice). Immunohistochemical analysis showed that ChR2-mCherry was expressed in VTA-dopamine neurons (Figure 2-1b). Next, I performed an in vivo microdialysis study to confirm the function of ChR2 in VTA-dopamine neurons. As a result, the dialysate dopamine levels in the N.Acc. were significantly increased by optical stimulation of the VTA in sham- and nerve-ligated mice (Figure 2-1c and d). Under these conditions, optical activation of VTA-dopamine neurons transiently reduced thermal hyperalgesia following sciatic nerve ligation. However, this effect was no longer evident at 2 hr after optical stimulation (Figure 2-1e to g).

Activation of mesolimbic dopamine neurons reversibly suppresses the allodynic effects of neuropathic and cancer pain

To specifically activate a mesolimbic dopaminergic pathway projecting from the VTA to the N.Acc. using optogenetics, I performed terminal stimulation in the N.Acc. of TH-cre/ChR2 mice. Immunohistochemical analysis showed that ChR2-mCherry was expressed in the N.Acc. in a subset of neurons expressing the dopamine transporter (DAT) (Figure 2-1h). Next, I performed an *in vivo* microdialysis study to confirm that optogenetic stimulation of ChR2 in VTA-dopamine neurons terminating in the N.Acc. resulted in an increase in dialysate dopamine (Figure 2-1i and j). Consistent with my results regarding the optical stimulation of VTA-dopamine neurons, optical activation of terminals in the N.Acc. suppressed the allodynic effect of sciatic nerve ligation (Figure 2-1k to m). Importantly, optogenetic activation of N.Acc. terminals did not produce any analgesic actions in sham-operated mice (Figure 2-1e and m).

I also investigated the effects of optical activation of VTA-dopamine neurons terminating in the N.Acc. on mouse model of tumor-induced bone pain. As a result, activation of mesolimbic dopaminergic neurons significantly suppressed the allodynia induced by intrafemoral bone marrow injection of osteosarcoma cells (Figure 2-2a to c).

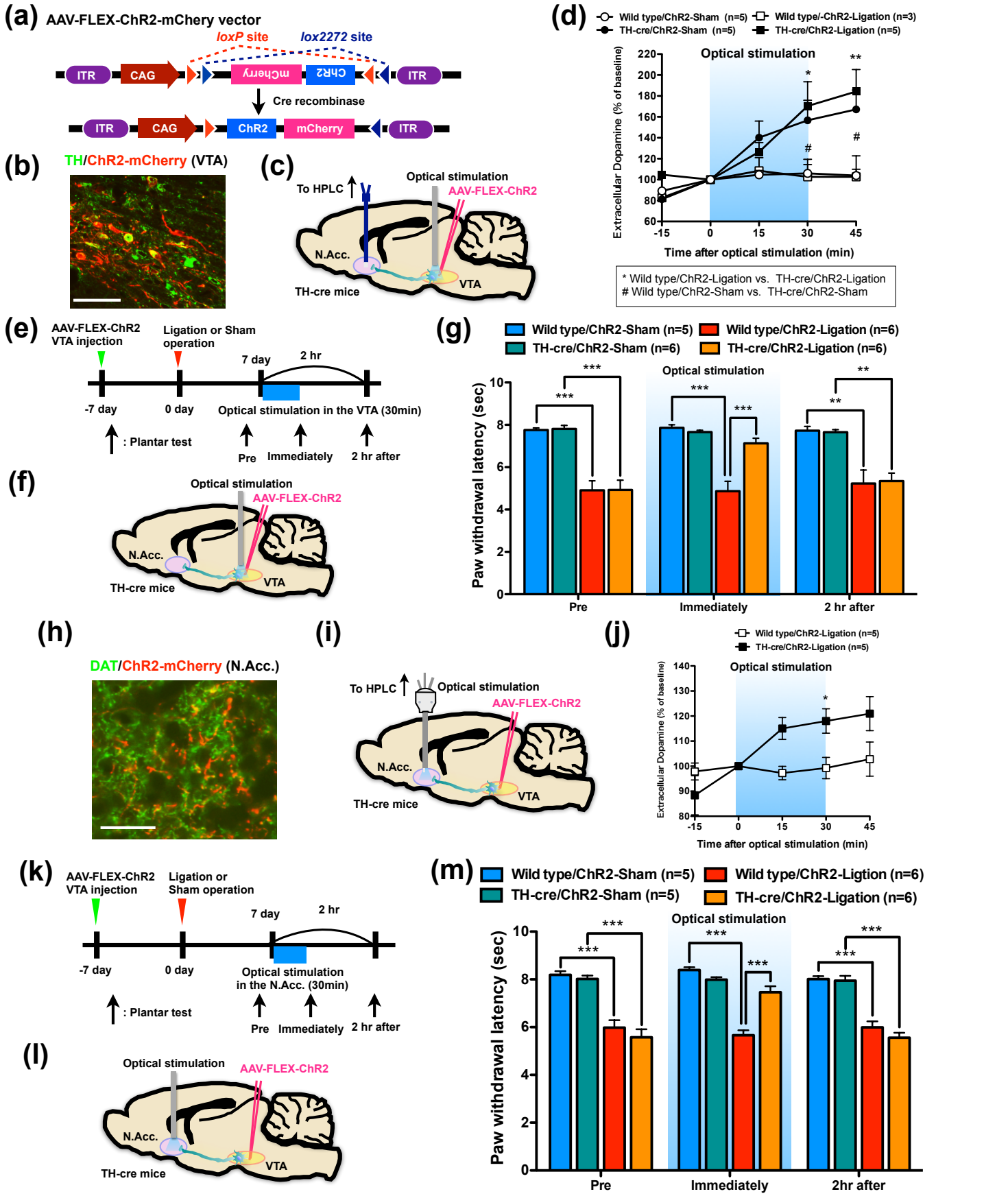

Figure 2-1

Activation of mesolimbic dopaminergic neurons projecting from the VTA to the N.Acc. reduces hyperalgesia following sciatic nerve ligation

(a) Construction of the Cre-dependent AAV. (b) Co-expression of ChR2-mCherry and TH. Scale bar = 50 μm. (c) Schematic of the experimental design. (d) Extracellular dopamine levels in the N.Acc. (n = 5, Wild type/ChR2-Sham; n = 3, Wild type/ChR2-Ligation; n = 5, TH-cre/ChR2-Sham; n = 5, TH-cre/ChR2-Ligation) (Wild type/ChR2-Sham vs. Wild type/ChR2-Ligation, $F_{4,24} = 0.14$; Wild type/ChR2-Sham vs. TH-cre/ChR2-Sham, $F_{4,32} = 5.47$; Wild type/ChR2-Ligation vs. TH-cre/ChR2-Ligation, $F_{4,24} = 4.09$). (e) Experimental timeline. (f) Schematic of the experimental design. (g) Paw-withdrawal latency in response to thermal stimulation (n = 5, Wild type/ChR2-Sham; n = 6, Wild type/ChR2-Ligation; n = 6, TH-cre/ChR2-Sham; n = 6, TH-cre/ChR2-Ligation). (h) Co-expression of ChR2-mCherry and DAT. Scale bar = 50 μm. (i) Schematic of the experimental design. (j) Extracellular dopamine levels in the N.Acc. of Wild type/ChR2-Ligation mice (n = 5) and TH-cre/ChR2-Ligation mice (n = 5, $F_{4,32} = 4.28$) (k) Experimental timeline. (l) Schematic of the experimental design. (m) Paw-withdrawal latency in response to thermal stimulation (n = 5, Wild type/ChR2-Sham; n = 6, Wild type/ChR2-Ligation; n = 5, TH-cre/ChR2-Sham; n = 6, TH-cre/ChR2-Ligation). Data are mean ± S.E.M. *p < 0.05; **p < 0.01; ***p < 0.001; #p < 0.05; by two-way repeated measures ANOVA with a Bonferroni post hoc analysis (d, j), one-way ANOVA with a Bonferroni post hoc analysis (g, m).

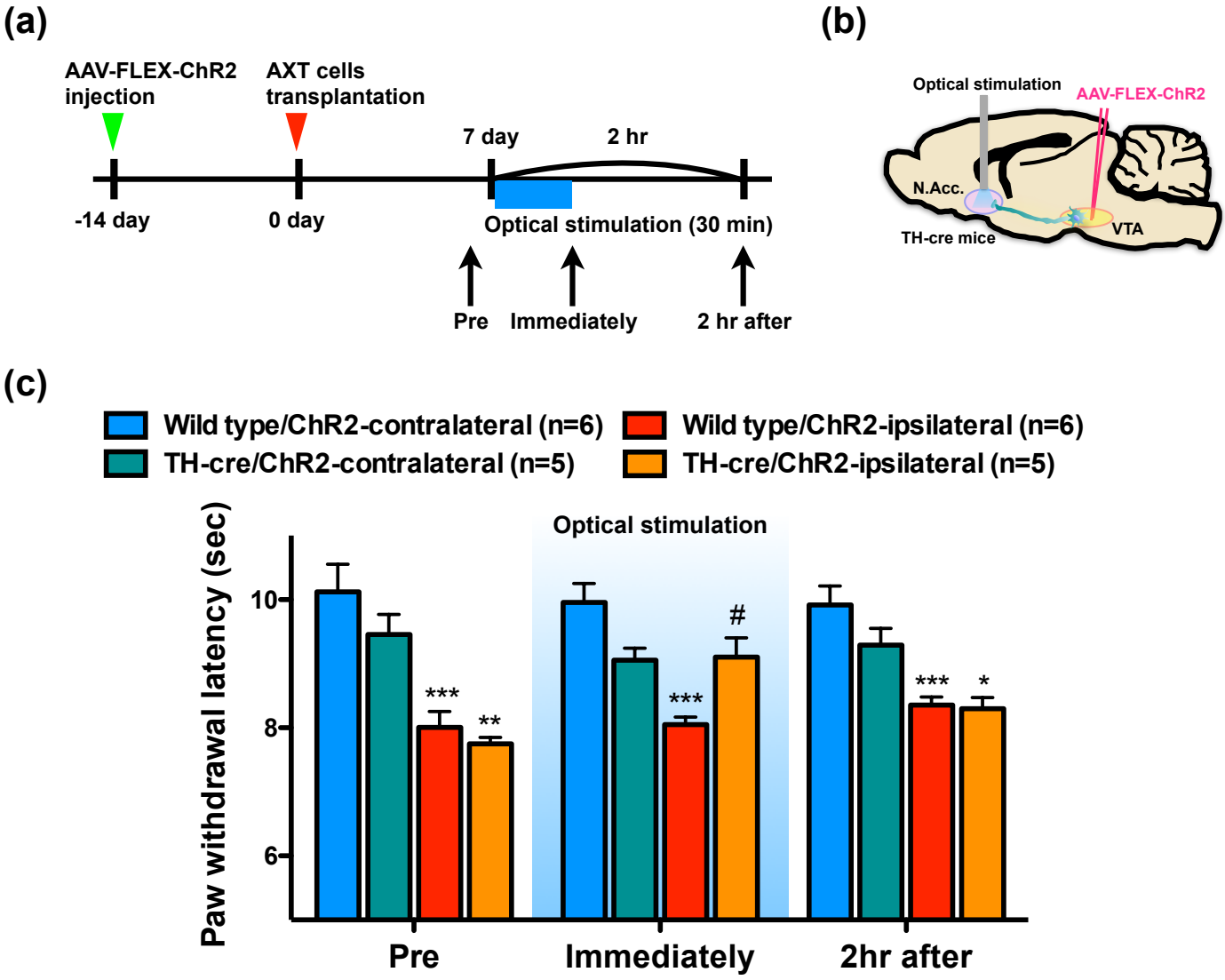

Figure 2-2

Activation of mesolimbic dopaminergic neurons projecting from the VTA to the N.Acc. reduces hyperalgesia following AXT cell transplantation into the femoral bone marrow cavity.

(a) Experimental timeline. (b) Schematic of the experimental design (c) Paw-withdrawal latency in response to thermal stimulation (n = 6, Wild type/ChR2-contralateral; n = 6, Wild type/ChR2-ipsilateral; n = 5, TH-cre/ChR2-contralateral; n = 5, TH-cre/ChR2-ipsilateral). Data are mean ± S.E.M. *$p < 0.05$, **$p < 0.01$, ***$p < 0.001$, #$p < 0.05$; by one-way ANOVA with a Bonferroni post hoc analysis (c).

Discussion

Many healthcare workers are faced with the difficulty of managing pain, including neuropathic and cancer-associated pain. Neuropathic pain is caused by injury or pathological changes in the peripheral or central nervous system. On the other hand, tumor-induced bone pain is the most common pain in patients with advanced cancer and the most common presenting symptom indicating that tumor cells have metastasized to sites beyond the primary tumor. Although the pain from bone metastases can be treated by multiple complementary approaches, bone cancer pain is still one of the most difficult chronic pains to fully control, since the efficacy of commonly used analgesics to treat bone cancer pain is often limited by significant adverse side effects. Moreover, little is known about the central mechanisms that promote bone cancer pain. In the present study, I revealed that specific activation of mesolimbic dopaminergic neurons alleviated neuropathic or bone cancer-induced pain. Previously Ren et al. showed that targeting a subpopulation of medium spiny neurons (MSNs) projecting from VTA dopaminergic neurons may enable the selective modulation of allodynia associated with these chronic pain states[50]. Importantly, my data also exhibited that the activation of VTA dopaminergic neurons does not influence the detection of physiological thermal pain. This finding is consistent with observations in human subjects that increasing levels of dopamine pharmacologically do not modulate the responses to noxious stimuli[74].

Thus, increased characterization of these VTA dopaminergic cells may enable the selective pharmacological modulation of pathological pain, without interfering with physiological pain or abnormal consequences of reward, including addiction.

Chapter 3

Extracellular N-acetylaspartylglutamate released in the nucleus accumbens modulates the pain sensation: analysis using a microdialysis/mass spectrometry integrated system

Introduction

Pain is a warning of potential tissue injury and functions to drive behavioral actions that result in protection of the body from further harm. Nociceptive signals engage broad neural networks in the brain including the thalamus, somatosensory, insula and cingulate cortices, the hypothalamus, amygdala, periaqueductal gray as well as the ventral striatum[61,75].

Various small molecules, including several amino acid (AA) derivatives and peptides, play roles in neural communication as not only classical neurotransmitters, but also neuromodulators[76], and their synaptic concentrations alter the excitability of specific neural circuits. As chronic pain alters neuronal excitability in the N.Acc.[61], I hypothesized that brain extracellular small molecules, including small peptides, as well as classical neurotransmitters play important roles in modulating the pain sensation. However, it is not easy to identify molecules having the potential to modulate pain owing to the absence of an analytical technique for comprehensively measuring brain extracellular metabolites.

In the present study, I applied a mass spectrometry (MS)-based metabolomics technique coupled with microdialysis to analyze extracellular metabolites released from cells in the brain and identified small molecules that are endogenously released in the N.Acc. for modulating pain and analgesia. This microdialysis/MS integration has also allowed monitoring of the changes in the extracellular metabolome during the application of pain

stimuli or the administration of analgesics. Among various MS methods, I used a recently established ion chromatography (IC) system together with Fourier transform high-resolution mass spectrometry (HRMS). Owing to the high chromatographic separation performance of IC for hydrophilic metabolites[77] and the high mass resolution of Orbitrap[78,79], this IC-HRMS approach allows the comprehensive detection of anionic metabolites in microdialyzed brain fluids, including nucleotides, organic acids, and small peptides[80,81]. These approaches therefore allowed us to identify N-acetylaspartylglutamate (NAAG) as an endogenously released transmitter in the N.Acc and to explore its relevance to modulation of nociception.

Materials and methods

Animals

Male C57BL/6J mice (8-12 weeks old) (Tokyo Laboratory Animals Science Co., Ltd., Tokyo, Japan) were housed up to 6 per cage and kept in a temperature-controlled room (24 ± 1°C). All mice were maintained under a 12 hr light-dark cycle (light on at 8 a.m.) and behavioral tests were performed during the light phase. Food and water were available *ad libitum*.

Drugs

Morphine hydrochloride (Daiichi-Sankyo Co., Ltd., Tokyo, Japan), N-acetyl-Asp-Glu (NAAG; Sigma-Aldrich, MO, USA), and PMPA (TOCRIS Bioscience, Bristol, UK) were used in this study. Morphine, NAAG and PMPA were dissolved in saline (Otsuka normal saline, 0.9% NaCl; Otsuka Pharmaceutical Factory Inc., Tokushima, Japan).

Artificial activation of sensory neurons by ChR2

(i) Virus vector

To achieve cell-type-specific ChR2 or enhanced green fluorescent protein (EGFP) expression, I used the adeno-associated virus serotype 6 (AAV6) vector with a human

synapsin 1 promoter (AAV-hSyn-ChR2 (ET/TC)-EYFP (AAV6-ChR2) or AAV-hSyn-EGFP (AAV6-EGFP)). Both virus vectors were serotyped with AAV6 coat proteins and packaged by the viral vector core at Nagoya University. The final viral concentration was 1×10^{11} and 3×10^{12} copies/mL. Aliquots of this virus were stored at -80°C until use.

(ii) AAV injection

To selectively express ChR2 or EGFP in sensory nerves, AAV6-ChR2 or AAV6-EGFP was microinjected into the sciatic nerve of C57BL/6J mice[18]. Briefly, mice were anesthetized under isoflurane (3%, inhalation). Sterilized forceps and scissors were used to make a 2-cm incision at the level of the sciatic nerve. The sciatic nerve was exposed by cutting the connective tissue. The AAV was microinjected through an internal cannula (Eicom, Kyoto, Japan) at 1 μL/min for 8 min (8 μL total volume) with a gas-tight syringe (10 μL; Eicom) and an air pressure injector system (Micro-syringe Pump-Model ESP-32; Eicom).

Measurement of the pain threshold

To quantify the change in sensitivity to a tactile stimulus induced by the optical activation of sensory nerves, paw withdrawal in response to a tactile stimulus during blue light stimulation (473 nm, continuous-wave; CW) of the plantar surface was measured using von Frey filaments with a bending force of 0.16 g (Aesthesio®, DanMic Global, LLC, San Jose, CA, USA). Each of the hind paws was tested individually. Paw withdrawal in response to a

tactile stimulus was evaluated by scoring as follows: 0, no response; 1, a slow and slight withdrawal response; 2, a slow and prolonged flexion withdrawal response (sustained lifting of the paw) to the stimulus; 3, a quick withdrawal response away from the stimulus without flinching or licking; 4, an intense withdrawal response away from the stimulus with brisk flinching and/or licking. Paw movements associated with locomotion or weight-shifting were not counted as a response. Before the behavioral responses to a tactile stimulus were tested, mice were habituated to their surroundings for 1 hr.

Immunohistochemistry

Mice were deeply anesthetized with 3% isoflurane (inhalation) and transcardially perfusion-fixed with 4% paraformaldehyde in 0.1 M phosphate-buffer (pH 7.4). Sciatic nerve and dorsal root ganglion were post-fixed and cryoprotected in 20-30 (w/v)% sucrose. Samples were then embedded in optimal cutting temperature compound (OTC compound; Tissue Tek; Sakura Fine Technical, Tokyo, Japan) and frozen sections were cut on a cryostat (CM1860; Leica Microsystems, Heidelberg, Germany) (8 μm). The brain sections were incubated in appropriate blocking solution and then with chicken monoclonal anti-GFP antibody (1:1000, abcam plc.), rabbit polyclonal anti-substance P antibody (1:800, Immunostar). Following washes, they were incubated with Alexa Fluor 488 goat anti-chicken antibody (1:400, Thermo Fisher Scientific), or Alexa Fluor 546 goat anti-rabbit antibody (1:10000, Thermo Fisher Scientific). For myelin staining, samples were incubated with FluoroMyelin Red (1:300,

#F34652, Thermo Fisher Scientific, MA, USA) for 20 min, and then rinsed in phosphate-buffered saline (PBS). The sections were mounted with Dako fluorescent mounting medium (Dako, Glostrup, Denmark). Fluorescence of immunolabeling was detected using a light microscope (BX-61; Olympus, Tokyo, Japan) and photographed with a digital camera (MD695; Molecular Devices, Sunnyvale, CA, USA).

MALDI-imaging

Two weeks after intrasciatic injection of AAV6-ChR2 or AAV6-EGFP, the mice expressing ChR2 or EGFP in sensory nerves were performed optical stimulation (473 nm, CW, 30 min) to the plantar surface of ipsilateral hind paw. Thirty minutes after optical stimulation, mice were sacrificed and whole brain was flash-frozen in solid CO_2 and stored at −80 °C.

Thin sections (8 μm thickness) were cut with a cryomicrotome (CM3050, Leica Microsystems) and thaw-mounted on an indium thin oxide-coated glass slide (Bruker Daltonics) at -16℃. After the sectioning, deuterium labeled dopamine (DA-d_4) as an internal standard (IS) was sprayed onto the sections by using a robotic sprayer device (SunCollect system, SunChrom, Friedrichsdorf, Germany). The sections were manually spray coated with 2,4-diphenyl-pyranylium (DPP) (1.3 mg/mL in methanol) using an artistic airbrush (Procon Boy FWA Platinum 0.2-mm caliber airbrush, Mr. Hobby, Tokyo, Japan) to employ on-tissue derivatization of the monoamines[82]. The sections were then automatically spray coated with

2,5-dihydroxybenzoic acid as a matrix (50 mg/mL, dissolved in 50% methanol) using the robotic sprayer. MALDI-IMS was performed using a linear ion trap MS with a MALDI source (MALDI LTQ XL, Thermo Fisher Scientific Inc.) equipped with a nitrogen laser (337 nm; 60 Hz). The laser energy and the raster step size were set at 32 μJ and 80 μm, respectively. During imaging measurements, signals of DPP-dopamine (*m/z* 368→232) and DPP-DA-d_4 (*m/z* 372→232) was monitored with a precursor ion isolation width of 1.0 *m/z* units. The obtained spectral data were then transformed to image data using ImageQuest 1.0.1 software (Thermo Fisher Scientific Inc.). Note that the dopamine signal was normalized by the IS (DA-d_4) signal simultaneously obtained from the same section.

In vivo microdialysis and sample collection

Mice were anesthetized by the inhalation of 3% isoflurane and placed in a small-animal stereotaxic instrument (RWD Life Science, CA, USA) for surgical implantation of a microdialysis guide cannula (CXG-6; Eicom). The microdialysis guide cannula with dummy probes (CXD-6; Eicom) was implanted into the N.Acc. (AP, +1.4 mm; AP, +1.5 mm; AP, -3.1 mm; angle, 10°). More than 6 days after implantation of the guide cannula, the dummy cannula was replaced by a microdialysis probe (CX-I-6-01; Eicom). The next day, the probe was continuously perfused with artificial cerebrospinal fluid (0.9 mM $MgCl_2$, 147.0 mM NaCl, 4.0 mM KCl, and 1.2 mM $CaCl_2$) at a flow rate of 1 μL/min by a syringe pump (ESP-32; Eicom) for at least 1 hr before sample collection. Outflow fractions were collected

every 30 min (30 min/fraction). After more than 2 baseline fractions were collected, mice were subjected to optical stimulation (activation of sensory nerves) or morphine injection (10 mg/kg, s.c.). Dialysis samples were stored at -80°C until use.

Quantification of metabolites by internal and external standards

I used both IS (added to the dialysates) and external standard (ES) compounds to determine *m/z* value and specific retention time in IC for all metabolites examined. The detailed method is as follows:

IS compounds

I used 2-morpholinoethanesulfonic acid (MES) as IS for anionic metabolites. The IS compound is not present in the brain fluids; thus, it serves as ideal standard. Loss of endogenous metabolites during sample preparation was corrected by calculating the recovery rate (%) for each sample measurement.

ES compounds

Before sample analysis, I measured the mixture of authentic compounds of target metabolites in ultrapure water to determine both *m/z* value and retention time of all metabolites examined.

Ion chromatography-tandem mass spectrometry for anionic metabolites.

For the analysis of small molecules released in the N.Acc induced by pain or the administration of analgesics, anionic metabolites were measured using an Orbitrap-type MS (Q-Exactive Focus; Thermo Fisher Scientific) connected to a high-performance ion-chromatography (IC) system (ICS-5000+; Thermo Fisher Scientific) that enables highly selective and sensitive metabolite quantification due to IC-separation and the Fourier-transform MS principle[77]. The IC was equipped with an anion electrolytic suppressor (Thermo Scientific Dionex AERS 500; Thermo Fisher Scientific) to convert the potassium hydroxide gradient into pure water before the sample entered the mass spectrometer. Separation was performed using a Thermo Scientific Dionex IonPac AS11-HC, with a 4-μm particle-size column. The IC flow rate of 0.25 mL/min was supplemented post-column with 0.18 mL/min makeup flow of MeOH. The potassium hydroxide gradient conditions for IC separation were as follows: from 1 mM to 100 mM (0–40 min), 100 mM (40–50 min), and 1 mM (50.1–60 min), at a column temperature of 30°C. The Q-Exactive Focus mass spectrometer was operated under an ESI negative mode for all detections. Full mass scan (*m/z* 70−900) was used at a resolution of 70,000. The automatic gain control target was set at 3×10^6 ions, and the maximum ion injection time was 100 ms. Source ionization parameters were optimized with a spray voltage of 3 kV, and other parameters were as follows: transfer temperature of 320°C, S-Lens level of 50, heater temperature of 300°C, Sheath gas at 36, and Aux gas at 10.

The hierarchical clustering algorithm in Eisen's software[83)] was applied to investigate the metabolite fluctuations before, during and after optogenetically induced pain as well as morphine induced analgesia.

Sustained infusion of NAAG or PMPA into the N.Acc.

Mice were anesthetized by the inhalation of 3% isoflurane and placed in a small-animal stereotaxic instrument for the surgical implantation of a microdialysis probe (D-I-6-01; Eicom). The microdialysis probe was directly implanted into the N.Acc. (AP, +1.4 mm; ML, ±1.5 mm; DV, -3.6 mm; angle, 10°). The next day, NAAG or PMPA was injected into the N.Acc. at a flow rate of 0.5 μl/min by a syringe pump (ESP-64; Eicom)

Statistical analysis

The data are presented as the mean ± S.E.M. or S.D. I chose the sample size based on similar publications in the field. The statistical significance of differences among the groups was assessed by Student's *t*-test (unpaired, two-tailed) or one-way ANOVA followed by the Bonferroni multiple comparisons test or. All statistical analyses were performed with GraphPad Prism 5.0 (GraphPad Software). A p value of < 0.05 was considered to reflect significance.

Results

Optical stimulation of channelrhodopsin-2-expressing sensory nerves induces pain-like behavior followed by N.Acc. specific dopamine reduction

In this study, I sought to identify brain extracellular molecules that are dynamically altered by the application of noxious stimulation or by the administration of analgesics. For this purpose, I needed to create an animal model in which nociceptive stimulation/relief could be induced within desired time-windows, as well as without the use of anesthetics. Therefore, I used an optogenetic approach to induce acute nociception[18]. I generated mice expressing channelrhodopsin-2 (ChR2) in sensory nerves with the injection of retrograde adeno-associated virus (AAV): AAV6-hSyn-ChR2 (ET/TC)-EGFP (Figure 3-1a). In this model, I could apply temporally controlled nociceptive stimulation by optogenetic neuronal activation.

Immunohistochemical analysis showed that ChR2-EYFP was expressed in cells containing substance P, a marker of nociceptive c-fiber neurons in the lumbar dorsal root ganglion (DRG) (Figure 3-1b). Additionally, ChR2-expressing axons of sciatic nerves were not found in myelinated A-fibers (Figure 3-1c). Exposure of the plantar surface of the ipsilateral hind paw with 473 nm blue light induced avoidance behaviors and reduced sensory thresholds consistent with the activation of nociceptors (Figure 3-1d).

Having generated the algesthesia inducible mouse, I then evaluated a biochemical effect of the pain in the N.Acc induced by optogenetic approach. Since dopamine in N.Acc. plays critical role for both nociceptive as well as analgesia inputs[73,84], thus, to demonstrate the efficacy of the optogenetic stimulation-induced pain, I assessed local dopamine concentration changes between ChR2-expressing noxious-stimulated and EGFP-expressing control animals. For this purpose, I employed an imaging mass spectrometry allowing in situ visualization of dopamine concentration (Figure 3-2). Strikingly, I found that tissue-content of dopamine was specifically reduced in the N.Acc. (Figure 3-2, arrowheads), but not caudoputamen (CP), demonstrating this noxious stimulation affects the N.Acc. dopamine metabolism.

Identification of small molecules released in the N.Acc. at concentrations oppositely respond to pain stimuli and analgesia

I collected dialysates in the N.Acc. before, during, and after the application of optogenetically induced pain and morphine-induced analgesia, and have presented the experimental timeline in Figures 3-3a and 3b, respectively. For pain analysis, dialysates were additionally collected in the prelimbic cortex (PL) to refine specific responders in the N.Acc. region.

I subsequently performed IC-HRMS in the negative ion detection mode and qualitatively identified more than 60 endogenous molecules in the dialysates. I could simultaneously trace their extracellular concentrations. Owing to the large dataset, I employed hierarchical

clustering, a multivariate analysis, which provided an overview of molecular fluctuations during the two perturbations (Figure 3-3).

As presented in Figure 3-3c, I found a group of molecules that exhibited N.Acc-specific reductions in response to pain stimuli as well as increases during analgesia. Focusing on this cluster, 12 metabolites, including amino acid derivatives (1 and 2), hexose and its metabolites (3, 6, 7, 9, and 12), a small peptide (4), a nucleotide precursor and decomposed product (5 and 8), and branched chain AA decomposed products (10 and 11), were identified. Finally, after statistical analysis (Figure 3-3d), the extracellular concentrations of NAAG and galactose-1-phosphate in the N.Acc. significantly responded to pain and analgesia in opposite manners (reduced by pain and elevated by analgesia; Figure 3-3e).

Infusion of NAAG in the N.Acc. modulates the pain threshold

After identifying NAAG and galactose-1-phosphate as candidates for endogenous pain modulation in the N.Acc., I proceeded to assess NAAG bioactivity for modulation of the pain sensation. NAAG is one of the most abundant neuro co-transmitters in the mammalian central nervous system and is known to be released from synaptic terminals[29,30,85]. On the other hand, galactose-1-phosphate is an intermediate in the intra-conversion of glucose and galactose, and there is limited information on its physiological role in the intercellular space. Therefore, I focused on NAAG and investigated the pain-modulating effects of the sustained infusion of NAAG into the N.Acc. (Figure 3-4a).

Interestingly, infusion of NAAG into the N.Acc. significantly attenuated pain induced by the optical activation of sensory nerves (Figure 3-4b). In the mammalian brain, NAAG is degraded to N-acetylaspartate (NAA) and glutamate by glutamate carboxypeptidase II (GCP-II)[34]. To confirm the effect of NAAG on the pain threshold and exclude the effect of its decomposed products, i.e., glutamate and NAA, I investigated the effect of infusion of a GCP-II inhibitor (2-(phosphonomethyl) pentanedioic acid [PMPA]) on the pain threshold. The infusion of PMPA into the N.Acc. attenuated the pain induced by the optical activation of sensory nerves as well as NAAG (Figure 3-4c), demonstrating that intact NAAG bioactivity could reduce acute pain.

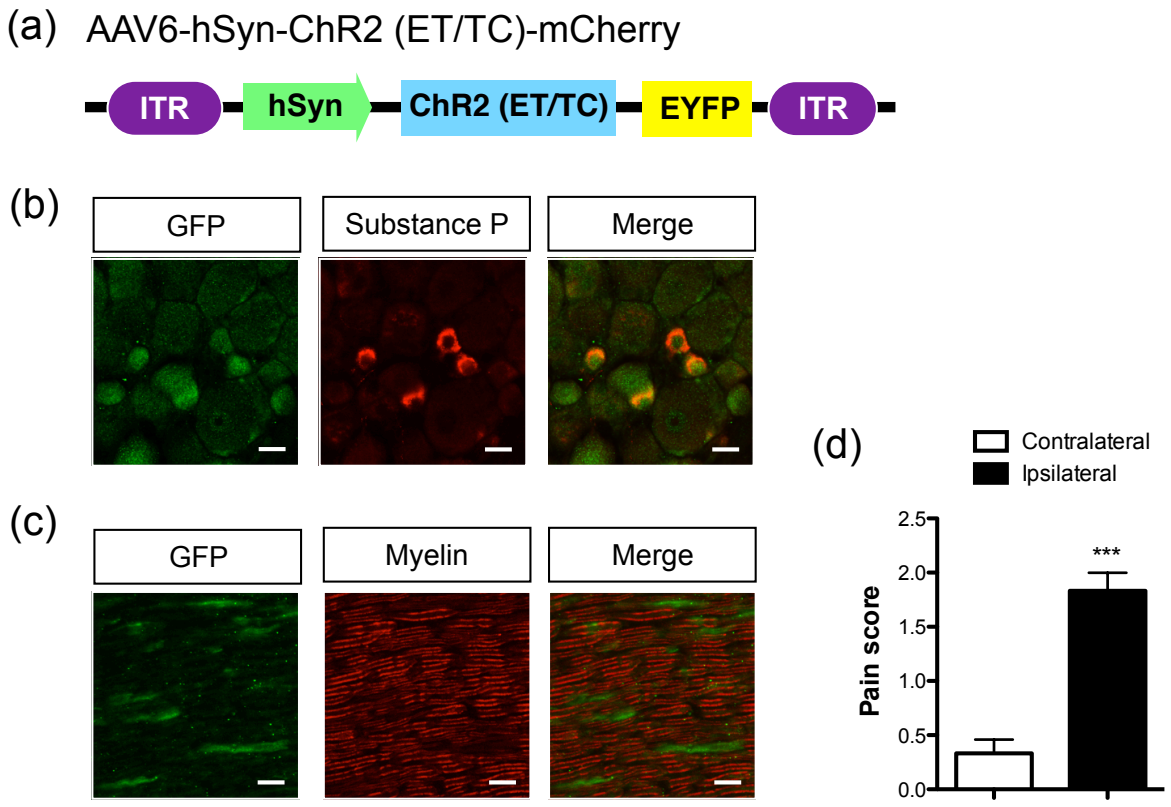

Figure 3-1

Effects of optical activation of sensory nerves on pain threshold

(a) Construct of the AAV. (b) Expression of ChR2 (ET/TC)-EYFP and Substance P in the lumber DRG (ipsilateral side). Scale bar = 20 μm. (c) Expression of ChR2 (ET/TC)-EYFP and myelin in the sciatic nerve. Scale bar = 20 μm. (d) von Frey thresholds in response to optical stimulation to the plantar ($n = 8$, $t(14) = 7.183$). Data are mean ± S.E.M. ***$p < 0.001$; by two-tailed Student's *t*-test.

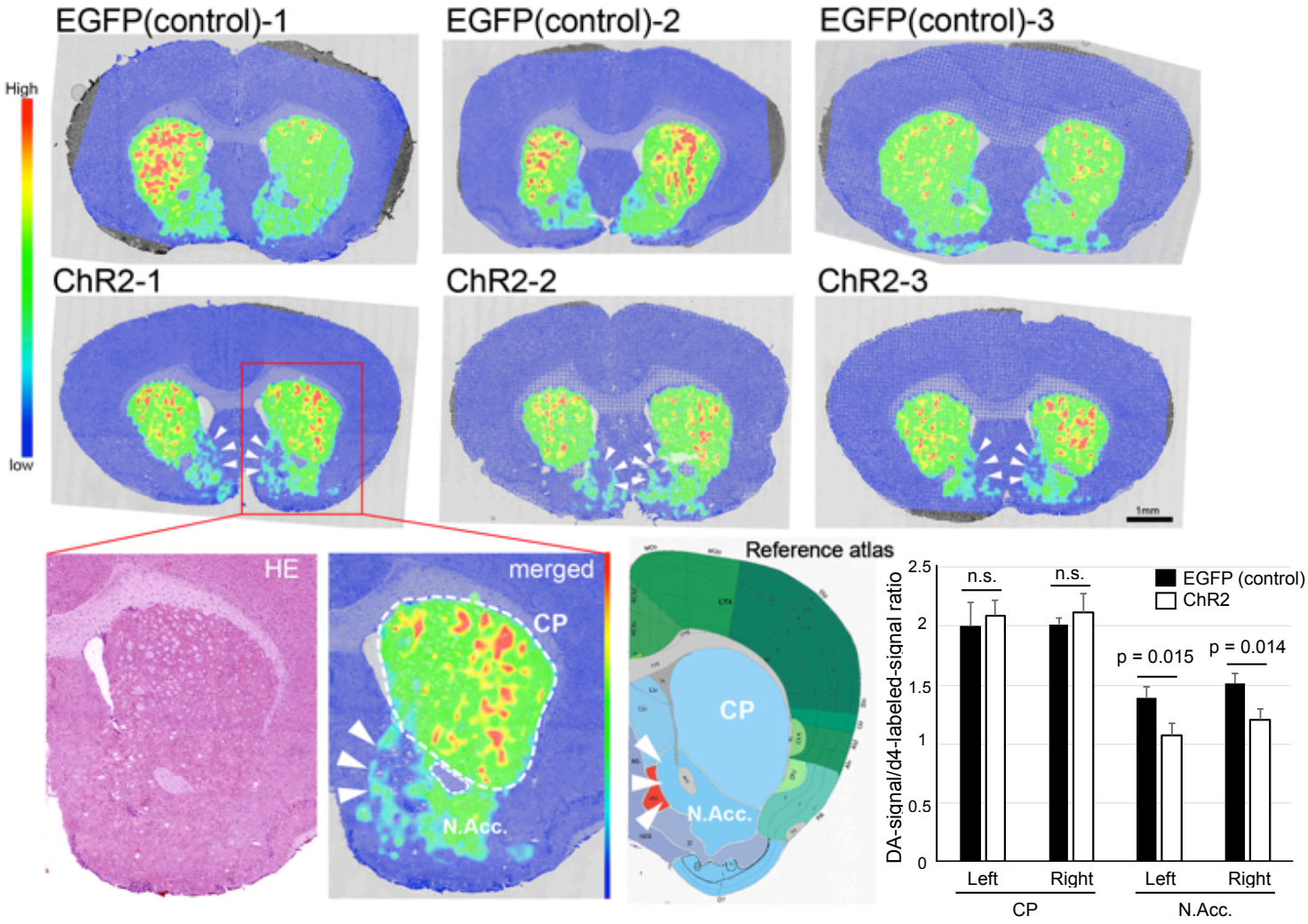

Figure 3-2

Visualization of dopamine concentration changes by optogenetic-stimulation in the mouse brain sections of noxious-stimulated mice. Imaging mass spectrometry visualized distribution of dopamine in coronal brain sections those contain N.Acc., from ChR2-expressing noxious-stimulated (middle) and EGFP-expressing control (upper) mice. Representative dopamine image of noxious-stimulated brain in high magnification and its corresponding reference atlas (Allen Brain Atlas, http://www.brain-map.org/) were also shown. Note that endogenous dopamine signal was normalized by an internal standard (deuterium labeled dopamine signal homogeneously spayed by a robotic sprayer device, see also methods). The normalized signal intensities from CP (Caudoputamen) and N.Acc. regions were quantified (lower right). Data are presented as mean ± S.D. *p < 0.05; by Student's *t*-test.

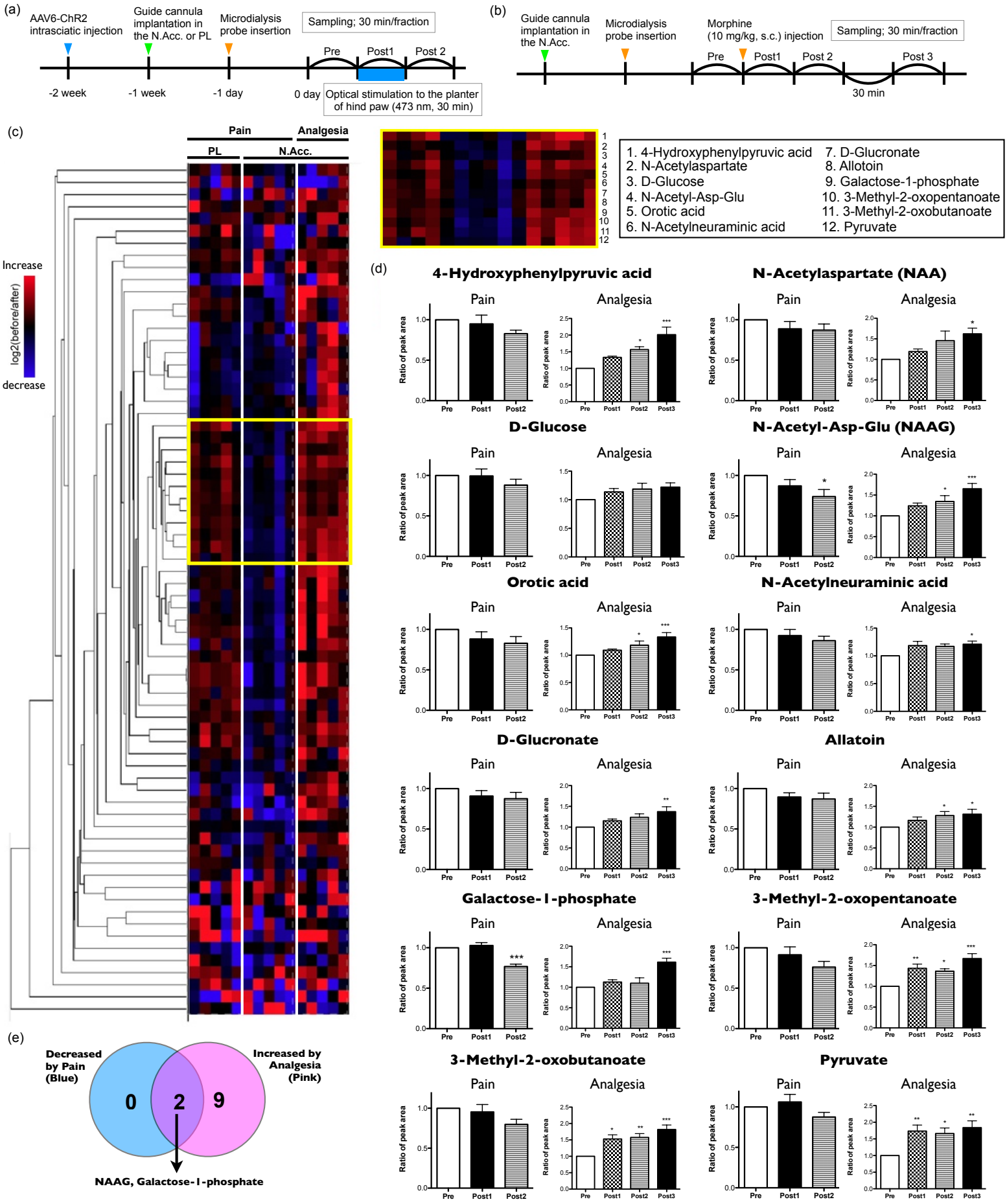

Figure 3-3

Profiling of dynamic changes of small molecules in the cerebral fluids of the N.Acc., in response to the optical activation of sensory nerves (pain stimuli) or systemic morphine injection (analgesia) by IC-HRMS analysis

(a, b) Experimental timeline of microdialysis experiment for mice with optogenetically induced pain (a) and morphine-induced analgesia (b). (c) Hierarchical clustering revealed a group of molecules shows up-regulation by pain stimuli in N.Acc., but not PL, and reduction by analgesia (yellow square). The clustering analysis was performed using log2 fold change values (pre/post). Red indicates increase and blue indicates decrease compared to the pre. (d) Time-course concentration changes of the clustered metabolites into the yellow square shown in (c). (e)The Venn diagram shows the number of decreased molecules by pain (blue) and increased molecules by analgesia (pink). Only NAAG and galactose-1-phosphate were identified as those significantly reduced by pain as well as elavated by analgesia. Data are mean ± S.E.M. *$p < 0.05$, **$p < 0.01$, ***$p < 0.001$; by one-way ANOVA with Bonferroni post hoc analysis.

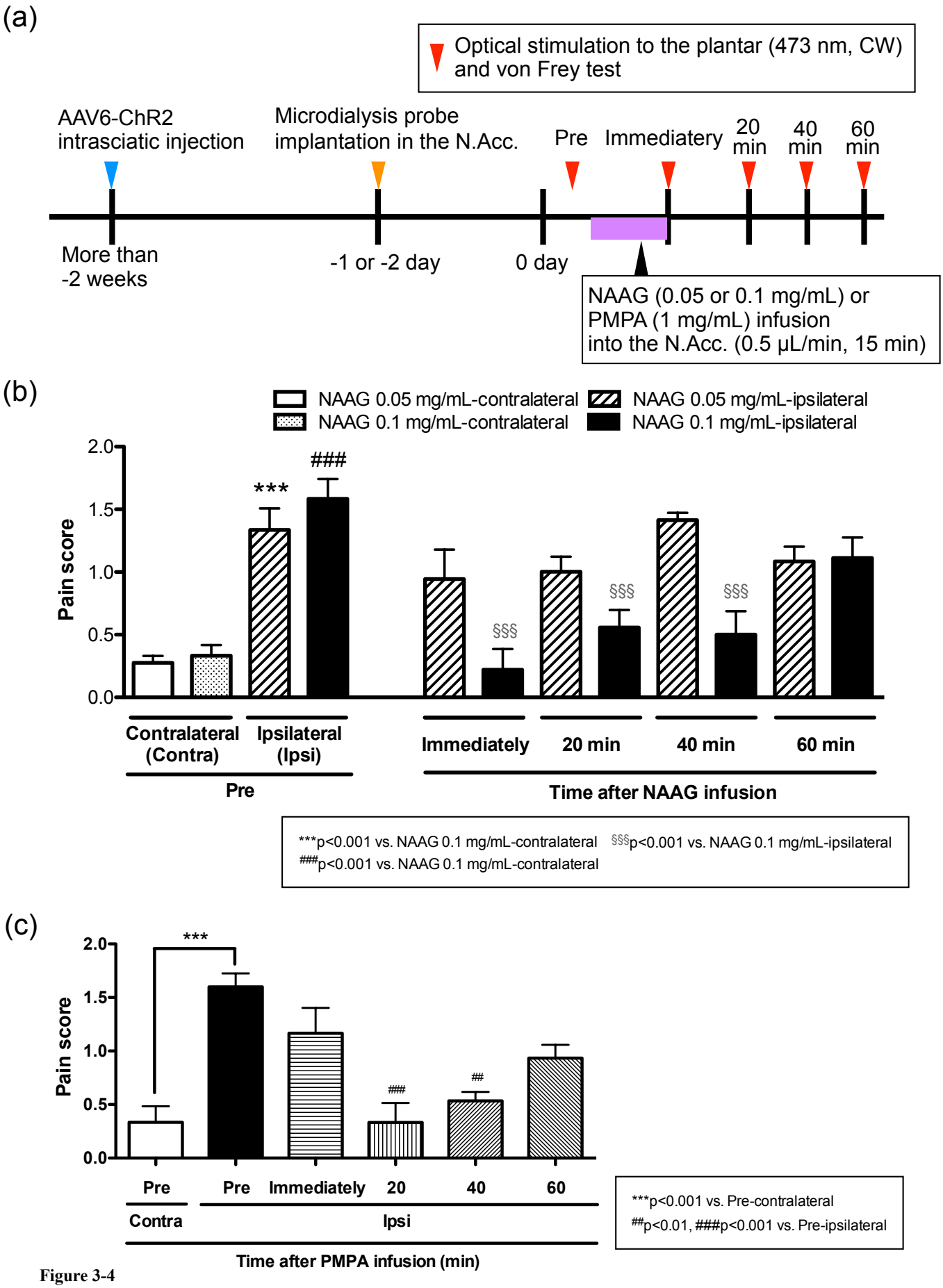

Figure 3-4

Effect of NAAG in the N.Acc. on optical activation of sensory nerves-mediated sensitivity to mechanical stimuli .

(a) Experimental timeline. (b, c) Effect of sustained infusion of NAAG (0.05 or 0.1 mg/mL, n = 6) (b) or PMPA (1 mg/mL, n = 5) (c) into the N.Acc. on pain score in response to optical activation of sensory nerves and von Frey filament. Data are mean ± S.E.M. ***$p < 0.001$, ## $p < 0.01$, ###$p < 0.001$, §§§$p < 0.001$; by one-way ANOVA with Bonferroni *post hoc* analysis.

Discussion

I performed a comprehensive analysis of small molecules that are released in the N.Acc. in response to activation of nociceptors or following administration of morphine as a analgesic. My goal was to identify, and begin to functionally characterize, potential neurotransmitter molecules relevant to pain in this brain region. Consequently, I detected over 60 metabolites in the N.Acc. and identified NAAG as a potential neurotransmitter relevant to pain and its modulation.

NAAG is considered to be a neurotransmitter that is mainly synthesized from NAA and glutamate in neurons[34], and is degraded to NAA and glutamate by NAAG peptidase (also known as glutamate carboxypeptidase II (GCPII)) on astrocytes or neurons[86]. NAAG has been suggested to act as an agonist for group II metabotropic glutamate receptors[36]. Furthermore, NAA in the dorsolateral prefrontal cortex and thalamus has been shown to be reduced under chronic pain[87,88]. Since NAAG derivatives in the brain may be reduced under chronic pain, I hypothesized that an increase in NAAG in the brain might produce analgesia. Consistent with this idea, increasing the level of NAAG by the inhibition of NAAG peptidase in the lateral ventricle, periaqueductal gray, rostral ventromedial medulla or locus coeruleus has been shown to produce analgesia[89-91]. Nevertheless, it was still unclear whether NAAG acted as a pain-modulator in the N.Acc. Therefore, I established an

animal model of pain using optogenetics, and investigated the pain-controlling effects of NAAG and PMPA. I found that the infusion of either NAAG or PMPA into the N.Acc. reduced nociceptive behaviors induced by the optical activation of sensory nerves.

It is worth to note that in my pain model, N.Acc. specific dopamine reduction was visualized by imaging mass spectrometry (Figure 3-2, arrow heads)[82]. Since it is reported that injection of NAAG as well as NAAG peptidase inhibitors lowered dopamine release in the N.Acc.[92,93], therefore, decreased extracellular NAAG concentration observed might accelerate a temporal dopamine release, its metabolism and finally lead shortage of dopamine content in the N.Acc. of my pain model. Although further studies are needed, these results suggest a linked regulation of NAAG and dopamine signaling in N.Acc., which might play an important role in the pain sensation.

In summary, using *in vivo* microdialysis coupled with an IC-HRMS technique, I found that NAAG is an endogenous pain modulator released in the N.Acc. Infusion of either NAAG or PMPA into the N.Acc. dramatically reduced pain induced by optical activation of sensory nerves. These results suggest that NAAG released in the N.Acc. could modulate the sensation of pain and may be a new target of drug discovery for predicting the ability to modulate pain.

General Conclusion

The above findings led to the following conclusions:

In Chapter 1:

In the present study, I investigated whether sciatic nerve injury or intrafemoral bone marrow injection of osteosarcoma affected the activity of mesolimbic dopaminergic neurons. I confirmed that sciatic nerve-injured and osteosarcoma-bearing mice exhibited allodynia in response to a thermal stimulus applied to the paw on the injured side. Under these conditions, I revealed that the intrinsic neuronal excitability of VTA dopamine neurons projecting to the N.Acc. was significantly reduced in these mice using patch-clamp electrophysiology techniques.

Taken together, these findings suggested that sustained afferent input from nerve injury and bone cancer may result in the suppression of mesolimbic dopaminergic neurons.

In Chapter 2:

I examined the possible contribution of the mesolimbic dopaminergic circuit to the modulation of allodynia related to neuropathic and cancer pain. To specifically activate mesolimbic dopaminergic neurons, I used optogenetic techniques. TH-cre mice that were microinjected with AAV to express ChR2 allowed the optogenetic stimulation of VTA

dopaminergic neurons in the VTA or in their N.Acc. terminals. I confirmed the activation of VTA dopaminergic neurons terminating in the N.Acc. through optical stimulation of ChR2 by an *in vivo* microdialysis study. Extracellular dopamine release in the N.Acc. was increased by optical stimulation of the VTA and N.Acc. Optogenetic activation of these cells produced significant but transient anti-allodynic effects in nerve-injured or tumor-bearing mice without increasing response thresholds to thermal stimulation in sham-operated animals.

These results indicated that the activity of mesolimbic dopaminergic neurons may contribute to modulate the neuropathic or cancer pain-induced allodynia, which may suggest strategies for modulating pathological pain states.

In Chapter 3:

I explored endogenous extracellular small molecules released in the N.Acc. with potential to modulate pain. To generate an animal model, which could induce nociceptive stimuli with the desired time-resolution, I used an optogenetic approach and assessed local changes in the dopamine concentration using IMS, which allowed *in situ* visualization of the dopamine concentration. Interestingly, the tissue content of dopamine was specifically reduced in the N.Acc. by an optogenetic approach to induce noxious stimulation. Next, I used an emerging metabolomics technique, IC-HRMS, and simultaneously analyzed the dynamics of more than 60 small molecules in brain fluids collected by microdialysis, under

both the application of pain stimuli induced by optogenetic methods and the administration of analgesics. Under these conditions, NAAG was identified as a potential endogenous pain-modulator released in the N.Acc. In addition, the infusion of NAAG into the N.Acc. significantly attenuated the pain induced by the activation of sensory nerves through optical stimulation.

Taken together, these findings, which were obtained using imaging mass spectrometry and *in vivo* microdialysis/mass spectrometry, suggested that dopamine and NAAG contribute to pain modulation.

In conclusion, the present study here demonstrated that the activity of mesolimbic dopaminergic neurons could modulate pathological pain, and NAAG released in the N.Acc. may, at least in part, contribute to this mechanism. Although further investigations are required, these results suggest that mesolimbic dopaminergic neurons and NAAG may be targets of drug discovery to identify new analgesics for pain relief.

List of Publications

1. Moe Watanabe, Michiko Narita, Yusuke Hamada, Akira Yamashita, Hideki Tamura, Daigo Ikegemi, Takashige Kondo, Tatsuto Shinzato, Takatsune Shimizu, Yumi Fukuchi, Akihiro Muto, Hideyuki Okano, Akihiro Yamanaka, Vivianne L. Tawfik, Naoko Kuzumaki, Edita Navratilova, Frank Porreca, Minoru Narita: Activation of VTA dopaminergic neurons reverses pathological allodynia resulting from nerve-injury or bone cancer. *Mol. Pain* (*Accepted*): **Chapter 1, 2**

2. Moe Watanabe, Yuki Sugiura, Eiji Sugiyama**,** Michiko Narita, Edita Navratilova, Takashige Kondo, Naohiko Uchiyama, Akihiro Yamanaka, Naoko Kuzumaki, Frank Porreca, Minoru Narita: Extracellular N-acetylaspartylglutamate released in the nucleus accumbens modulates the pain sensation: analysis using a microdialysis/mass spectrometry integrated system. *Mol. Pain (Accepted)*: **Chapter 3**

Acknowledgements

This research will never be materialized without the help of the following people and organization:

First, I would like to express my gratitude and appreciation to Professor Minoru Narita (Department of Pharmacology, School of Pharmacy and Pharmaceutical Science, Hoshi University) for his helpful guidance in my work and preparing this dissertation, and for giving a chance of this research work.

I would like to thank Ms. Michiko Narita (Department of Pharmacology) for her excellent technical assistance, helpful guidance, and valuable advices for my research work.

I would like to thank Dr. Naoko Kuzumaki (Lecturer, Department of Pharmacology) for stimulating discussions and kindly guidance in my research work.

I would like to thank Dr. Tomohisa Mori (Professor, Department of Pharmacology), Dr. Masahiro Shibasaki (Lecturer, Department of Pharmacology) and Miho Kawata (Assistant Professor, Department of Pharmacology) for critical comments and advises in my research work.

I would like to thank Professor Frank Porreca (Department of Pharmacology, University of Arizona) and Dr. Edita Navratilova (Department of Pharmacology, University of

Arizona) for their valuable discussion and helpful guidance in my research work.

I would like to thank Dr. Yuki Sugiura (Department of Biochemistry, Keio University School of Medicine) for his excellent technical assistance and valuable discussion in my research work, and for giving a chance of this research work.

I would like to thank Dr. Hideki Tamura (Life Science Tokyo Advanced Research Center (L-StaR), Hoshi University), Dr. Akira Yamashita (Department of Physiology, Kagoshima University) and Dr. Hiroyuki Tezuka (L-StaR, Hoshi University), for their excellent technical assistance, stimulating discussion and helpful guidance in my research work.

I would like to thank Dr. Daigo Ikegami (Department of Pharmacology, University of Arizona), Dr. Eiji Sugiyama (Department of Biochemistry, Keio University School of Medicine), Dr. Takatsune Shimizu (Department of Pathophysiology, Hoshi University), Professor Akihiro Muto (Department of Pathophysiology, Hoshi University) and Dr. Yumi Fukuchi (Department of Pathophysiology, Hoshi University) for their excellent technical assistance and helpful guidance in my research work.

I would like to thank Professor Emiko Senba (Department of Physical Therapy, Osaka Yukioka College of Health Science), Professor Hideyuki Okano (Department of Physiology, Keio University), Professor Akihiro Yamanaka (Department of Neuroscience II, Nagoya University), Dr. Katsuhide Igarashi (L-StaR, Hoshi University), Dr. Yoshinori Kato (L-StaR, Hoshi University), Ms. Maky Ohtsuka (L-StaR, Hoshi University), Dr. Naoki Yamamoto (L-StaR, Hoshi University), Dr. Hiroyasu Sakai (Department of Analytical

Pathophysiology, Hoshi University), Professor Hidemasa Furue (Department of Neurophysiology, Hyogo College of Medicine), Professor Kazunobu Sawamoto (Developmental & Regenerative Biology, Nagoya City University), Dr. Naoko Kaneko (Developmental & Regenerative Biology, Nagoya City University) and Dr. Kanako Nakaguchi (Developmental & Regenerative Biology, Nagoya City University) for their great technical suggestions in my research work.

I wish to thank Dr. Yusuke Hamada for his stimulating discussions and kindly supports in my research work.

I wish to thank Mr. Takashige Kondo, Ms. Chizuru Iwasawa and Ms. Yukari Suda for their helpful technical assistance and kindly supports in my research work.

I wish to thank Dr. Hiroshi Horiuchi, Mr. Akitoshi Date, Ms. Atsumi Nagasawa, Mr. Makoto Yanase and Dr. Atsunobu Sagara for their stimulating discussions and kindly technical assistance in my research.

I wish to thank Ms. Eri Shimura, Ms. Maki Noguchi and Mr. Yuki Suhara for their helpful technical and kindly supports in my research work.

I wish to thank Mr. Tatsuto Shinzato, Mr. Hidetsugu Ogata, Mr. Naohiko Uchiyama, Mr. Yoshitaka Iwayama, Mr. Daisuke Sato, Ms. Yuki Sudo, Mr. Shogo Uo, Mr. Shogo Miyazaki, Ms. Kayo Yasuda, Ms. Natsumi Yokoyama, Mr. Riku Tojo, Ms. Yuria Hayashi, Ms. Hinata Umino, Mr. Shinya Kimura, Mr. Jun Nakao, Ms. Eri Furuta for their great technical assistance in my research work and kindly encouragement to me.

I wish to thank Dr. Aya Maekawa, Mr. Kazuhiko Arakawa, Ms. Seira Doi, Ms. Toshihisa Nakajima, Mr. Toshimasa Ito, Mr. Yoshiyuki Iwase, Mr. Masato Uda, Dr. Yosuke Katsuta, Dr. Takao Tamagawa, Dr. Cheolsun Han, Dr. Fukiko Matsuyama, Ms. Mamiko Mantani, Dr. Yoshiyuki Meguro, Ms. Sachiko Arai, Dr. Yuya Ise, Dr. Hisakatsu Ito, Dr. Masahiko Odo, Dr. Keito Koh, Mr. Takahide Koda, Dr. Tomohiko Takada, Dr. Naosuke Hori, Dr. Kenta Wakaizumi, Ms. Masako Wakita, Dr. Yoshinori Takemura, Dr. Tatsuya Enomoto, Dr. Hironori Saisu, Dr. Shigeto Hirayama, Dr. Kenjiro Matsumoto, and Mr. Shota Morikawa for their stimulating discussions and useful guidance in my research work.

I wish to thank Mr. Toshiki Aiuchi, Mr. Kenichi Tanaka, Mr. Daisuke Oikawa, Ms. Mamiko Sakaki, Ms. Mina Kitagawa, Mr. Ryosuke Shinkai, Mr. Yuki Sanbongi, Mr. Takashi Kawamura and Ms. Yuka Miyake for their helpful supports in my research work and kindly encouragement to me.

Also, I wish to thank Ms. Megumi Aoki, Ms. Saaya Akamatsu, Ms. Risa Arai, Mr. Yuya Igeta, Ms. Hanae Ishimi, Mr. Wataru Ito, Mr. Hideto Kazamatsuri, Mr. Tomoya Koike, Mr. Akihiro Kodama, Ms. Chihiro Goto, Ms. Rei Sugiura, Ms. Mio Sekiguchi, Mr. Ryunosuke Tateishi, Ms. Masako Nagai, Mr. Hiroki Narita, Ms. Akane Hayashi, Ms. Ayaka Honda, Ms. Yuri Fujimori, Ms. Airi Mizukami, Ms. Akiko Miyazaki, Ms. Mikiko Mori, Ms. Mutsumi Yamashita, Ms. Reona Asano, Mr. Yuki Adachi, Ms. Yuka Ishibashi, Mr. Morinao Itoman, Ms. Yuko Oka, Ms. Naomi Kanao, Ms. Miyu Koizumi, Mr. Masahiro Sasaki, Mr. Shohei Sugai, Ms. Rino Sugata, Ms. Shuko Suzuki, Ms. Moe Nakahama, Ms.

Miho Nanbu, Ms. Ayana Nieda, Ms. Sara Yoshida, Ms. Yuki Yoneyama, Ms. Junna Wada, Mr. Katsunori Asano, Ms. Reiko Kagawa and Ms. Haruka Mikata, Ms. Yuri Ikeda, Mr. Yusuke Ishigami, Ms. Kurumi Itagaki, Mr. Yusuke Iwazawa, Mr. Kotaro Oikawa, Ms. Mariko Kobayashi, Mr. Kiwamu Sakurai, Ms. Asami Shinohara, Mr. Ken Takami, Mr. Kazuki Tanabe, Ms. Riko Morito, Ms. Mai Yamaguchi, Mr. Ryosuke Wakai, Ms. Hanako Akimoto, Ms. Moe Adachi, Mr. Haruki Ishiwata, Mr. Yuto Ota, Mr. Masayuki Otsubo, Mr. Takumu Omori, Ms. Arisa Gina, Ms. Saaya Kojima, Mr. Ko Takahashi, Ms. Mayu Tsujimura, Mr. Hisao Tsutsui, Mr. Yoshikazu Tominaga, Ms. Kyoka Higuchi, Ms. Saki Hirahara, Ms. Anna Hori, Mr. Hitoshi Makabe, Ms. Misa Matsufuji, Mr. Takaaki Mizuno, Ms. Akiko Yasumoto, Mr. Yuto Kaminogo, Mr. Hiroaki Matsumoto, Ms. Risa Matsumoto, Mr. Yamabe Yoshiyuki and Ms. Risa Takahashi for their supports.

Finally, I would like to express my deepest gratitude to my parents, my sister and many fiends for their assistance in my life.

References

1. Mantyh, P. (2013) Bone cancer pain: causes, consequences, and therapeutic opportunities. *Pain* **154 Suppl 1**, S54-62
2. Bromberg-Martin, E. S., Matsumoto, M., and Hikosaka, O. (2010) Dopamine in motivational control: rewarding, aversive, and alerting. *Neuron* **68**, 815-834
3. Adcock, R. A., Thangavel, A., Whitfield-Gabrieli, S., Knutson, B., and Gabrieli, J. D. (2006) Reward-motivated learning: mesolimbic activation precedes memory formation. *Neuron* **50**, 507-517
4. Berridge, K. C. (2007) The debate over dopamine's role in reward: the case for incentive salience. *Psychopharmacology (Berl)* **191**, 391-431
5. Brischoux, F., Chakraborty, S., Brierley, D. I., and Ungless, M. A. (2009) Phasic excitation of dopamine neurons in ventral VTA by noxious stimuli. *Proc Natl Acad Sci U S A* **106**, 4894-4899
6. Salamone, J. D., and Correa, M. (2012) The mysterious motivational functions of mesolimbic dopamine. *Neuron* **76**, 470-485
7. Schultz, W. (2002) Getting formal with dopamine and reward. *Neuron* **36**, 241-263
8. Lammel, S., Lim, B. K., and Malenka, R. C. (2014) Reward and aversion in a heterogeneous midbrain dopamine system. *Neuropharmacology* **76 Pt B**, 351-359
9. Grace, A. A., and Bunney, B. S. (1984) The control of firing pattern in nigral dopamine neurons: single spike firing. *J Neurosci* **4**, 2866-2876
10. Bayer, H. M., and Glimcher, P. W. (2005) Midbrain dopamine neurons encode a quantitative reward prediction error signal. *Neuron* **47**, 129-141
11. Mirenowicz, J., and Schultz, W. (1996) Preferential activation of midbrain dopamine neurons by appetitive rather than aversive stimuli. *Nature* **379**, 449-451
12. Deisseroth, K., Feng, G., Majewska, A. K., Miesenböck, G., Ting, A., and Schnitzer, M. J. (2006) Next-generation optical technologies for illuminating genetically targeted brain circuits. *J Neurosci* **26**, 10380-10386

13. Deisseroth, K. (2011) Optogenetics. *Nat Methods* **8**, 26-29

14. Deisseroth, K. (2015) Optogenetics: 10 years of microbial opsins in neuroscience. *Nat Neurosci* **18**, 1213-1225

15. Sauer, B., and Henderson, N. (1988) Site-specific DNA recombination in mammalian cells by the Cre recombinase of bacteriophage P1. *Proc Natl Acad Sci U S A* **85**, 5166-5170

16. Sternberg, N., and Hamilton, D. (1981) Bacteriophage P1 site-specific recombination. I. Recombination between loxP sites. *J Mol Biol* **150**, 467-486

17. Schnütgen, F., Doerflinger, N., Calléja, C., Wendling, O., Chambon, P., and Ghyselinck, N. B. (2003) A directional strategy for monitoring Cre-mediated recombination at the cellular level in the mouse. *Nat Biotechnol* **21**, 562-565

18. Iyer, S. M., Montgomery, K. L., Towne, C., Lee, S. Y., Ramakrishnan, C., Deisseroth, K., and Delp, S. L. (2014) Virally mediated optogenetic excitation and inhibition of pain in freely moving nontransgenic mice. *Nat Biotechnol* **32**, 274-278

19. Towne, C., Schneider, B. L., Kieran, D., Redmond, D. E., and Aebischer, P. (2010) Efficient transduction of non-human primate motor neurons after intramuscular delivery of recombinant AAV serotype 6. *Gene Ther* **17**, 141-146

20. San Sebastian, W., Samaranch, L., Heller, G., Kells, A. P., Bringas, J., Pivirotto, P., Forsayeth, J., and Bankiewicz, K. S. (2013) Adeno-associated virus type 6 is retrogradely transported in the non-human primate brain. *Gene Ther* **20**, 1178-1183

21. Towne, C., Pertin, M., Beggah, A. T., Aebischer, P., and Decosterd, I. (2009) Recombinant adeno-associated virus serotype 6 (rAAV2/6)-mediated gene transfer to nociceptive neurons through different routes of delivery. *Mol Pain* **5**, 52

22. Berry, K. A., Hankin, J. A., Barkley, R. M., Spraggins, J. M., Caprioli, R. M., and Murphy, R. C. (2011) MALDI imaging of lipid biochemistry in tissues by mass spectrometry. *Chem Rev* **111**, 6491-6512

23. Benabdellah, F., Touboul, D., Brunelle, A., and Laprévote, O. (2009) In situ primary metabolites localization on a rat brain section by chemical mass spectrometry imaging. *Anal Chem* **81**, 5557-5560

24. Hsieh, Y., Chen, J., and Korfmacher, W. A. (2007) Mapping pharmaceuticals in

tissues using MALDI imaging mass spectrometry. *J Pharmacol Toxicol Methods* **55**, 193-200

25. Cornett, D. S., Frappier, S. L., and Caprioli, R. M. (2008) MALDI-FTICR imaging mass spectrometry of drugs and metabolites in tissue. *Anal Chem* **80**, 5648-5653
26. Khatib-Shahidi, S., Andersson, M., Herman, J. L., Gillespie, T. A., and Caprioli, R. M. (2006) Direct molecular analysis of whole-body animal tissue sections by imaging MALDI mass spectrometry. *Anal Chem* **78**, 6448-6456
27. Inoue, K. (2009) Neurotransmitter. In *Encyclopedia of Neuroscience* (Binder, M. D., Hirokawa, N., and Windhorst, U., eds) pp. 2834-2834, Springer Berlin Heidelberg, Berlin, Heidelberg
28. M. Cowan, W. a. R. K. E. (2001) A brief history of synapses and synaptic transmission.
29. Neale, J. H., Bzdega, T., and Wroblewska, B. (2000) N-Acetylaspartylglutamate: the most abundant peptide neurotransmitter in the mammalian central nervous system. *J Neurochem* **75**, 443-452
30. Coyle, J. T. (1997) The nagging question of the function of N-acetylaspartylglutamate. *Neurobiol Dis* **4**, 231-238
31. Gehl, L. M., Saab, O. H., Bzdega, T., Wroblewska, B., and Neale, J. H. (2004) Biosynthesis of NAAG by an enzyme-mediated process in rat central nervous system neurons and glia. *J Neurochem* **90**, 989-997
32. Cangro, C. B., Namboodiri, M. A., Sklar, L. A., Corigliano-Murphy, A., and Neale, J. H. (1987) Immunohistochemistry and biosynthesis of N-acetylaspartylglutamate in spinal sensory ganglia. *J Neurochem* **49**, 1579-1588
33. Arun, P., Madhavarao, C. N., Moffett, J. R., and Namboodiri, M. A. (2006) Regulation of N-acetylaspartate and N-acetylaspartylglutamate biosynthesis by protein kinase activators. *J Neurochem* **98**, 2034-2042
34. Becker, I., Lodder, J., Gieselmann, V., and Eckhardt, M. (2010) Molecular characterization of N-acetylaspartylglutamate synthetase. *J Biol Chem* **285**, 29156-29164
35. Collard, F., Stroobant, V., Lamosa, P., Kapanda, C. N., Lambert, D. M., Muccioli, G.

G., Poupaert, J. H., Opperdoes, F., and Van Schaftingen, E. (2010) Molecular identification of N-acetylaspartylglutamate synthase and beta-citrylglutamate synthase. *J Biol Chem* **285**, 29826-29833

36. Wroblewska, B., Wroblewski, J. T., Pshenichkin, S., Surin, A., Sullivan, S. E., and Neale, J. H. (1997) N-acetylaspartylglutamate selectively activates mGluR3 receptors in transfected cells. *J Neurochem* **69**, 174-181

37. Wroblewska, B., Wroblewski, J. T., Saab, O. H., and Neale, J. H. (1993) N-acetylaspartylglutamate inhibits forskolin-stimulated cyclic AMP levels via a metabotropic glutamate receptor in cultured cerebellar granule cells. *J Neurochem* **61**, 943-948

38. Wroblewska, B., Santi, M. R., and Neale, J. H. (1998) N-acetylaspartylglutamate activates cyclic AMP-coupled metabotropic glutamate receptors in cerebellar astrocytes. *Glia* **24**, 172-179

39. McWilliams, L. A., Cox, B. J., and Enns, M. W. (2003) Mood and anxiety disorders associated with chronic pain: an examination in a nationally representative sample. *Pain* **106**, 127-133

40. Berger, A., Dukes, E. M., and Oster, G. (2004) Clinical characteristics and economic costs of patients with painful neuropathic disorders. *J Pain* **5**, 143-149

41. D'Ardenne, K., McClure, S. M., Nystrom, L. E., and Cohen, J. D. (2008) BOLD responses reflecting dopaminergic signals in the human ventral tegmental area. *Science* **319**, 1264-1267

42. Seltzer, Z., Dubner, R., and Shir, Y. (1990) A novel behavioral model of neuropathic pain disorders produced in rats by partial sciatic nerve injury. *Pain* **43**, 205-218

43. Malmberg, A. B., and Basbaum, A. I. (1998) Partial sciatic nerve injury in the mouse as a model of neuropathic pain: behavioral and neuroanatomical correlates. *Pain* **76**, 215-222

44. Shimizu, T., Ishikawa, T., Sugihara, E., Kuninaka, S., Miyamoto, T., Mabuchi, Y., Matsuzaki, Y., Tsunoda, T., Miya, F., Morioka, H., Nakayama, R., Kobayashi, E., Toyama, Y., Kawai, A., Ichikawa, H., Hasegawa, T., Okada, S., Ito, T., Ikeda, Y.,

Suda, T., and Saya, H. (2010) c-MYC overexpression with loss of Ink4a/Arf transforms bone marrow stromal cells into osteosarcoma accompanied by loss of adipogenesis. *Oncogene* **29**, 5687-5699

45. Niikura, K., Narita, M., Nakamura, A., Okutsu, D., Ozeki, A., Kurahashi, K., Kobayashi, Y., Suzuki, M., and Suzuki, T. (2008) Direct evidence for the involvement of endogenous beta-endorphin in the suppression of the morphine-induced rewarding effect under a neuropathic pain-like state. *Neurosci Lett* **435**, 257-262
46. Lindvall, O., and Björklund, A. (1974) The organization of the ascending catecholamine neuron systems in the rat brain as revealed by the glyoxylic acid fluorescence method. *Acta Physiol Scand Suppl* **412**, 1-48
47. Lindvall, O., Björklund, A., Moore, R. Y., and Stenevi, U. (1974) Mesencephalic dopamine neurons projecting to neocortex. *Brain Res* **81**, 325-331
48. Swanson, L. W. (1982) The projections of the ventral tegmental area and adjacent regions: a combined fluorescent retrograde tracer and immunofluorescence study in the rat. *Brain Res Bull* **9**, 321-353
49. Ozaki, S., Narita, M., Iino, M., Sugita, J., Matsumura, Y., and Suzuki, T. (2002) Suppression of the morphine-induced rewarding effect in the rat with neuropathic pain: implication of the reduction in mu-opioid receptor functions in the ventral tegmental area. *J Neurochem* **82**, 1192-1198
50. Ren, W., Centeno, M. V., Berger, S., Wu, Y., Na, X., Liu, X., Kondapalli, J., Apkarian, A. V., Martina, M., and Surmeier, D. J. (2016) The indirect pathway of the nucleus accumbens shell amplifies neuropathic pain. *Nat Neurosci* **19**, 220-222
51. Loggia, M. L., Berna, C., Kim, J., Cahalan, C. M., Gollub, R. L., Wasan, A. D., Harris, R. E., Edwards, R. R., and Napadow, V. (2014) Disrupted brain circuitry for pain-related reward/punishment in fibromyalgia. *Arthritis Rheumatol* **66**, 203-212
52. Steinberg, E. E., and Janak, P. H. (2013) Establishing causality for dopamine in neural function and behavior with optogenetics. *Brain Res* **1511**, 46-64
53. Stubbs, B., Thompson, T., Acaster, S., Vancampfort, D., Gaughran, F., and Correll, C. U. (2015) Decreased pain sensitivity among people with schizophrenia: a

meta-analysis of experimental pain induction studies. *Pain* **156**, 2121-2131

54. Blanchet, P. J., and Brefel-Courbon, C. (2017) Chronic pain and pain processing in Parkinson's disease. *Prog Neuropsychopharmacol Biol Psychiatry*

55. Maeda, T., Shimo, Y., Chiu, S. W., Yamaguchi, T., Kashihara, K., Tsuboi, Y., Nomoto, M., Hattori, N., Watanabe, H., Saiki, H., and group, J.-F. (2017) Clinical manifestations of nonmotor symptoms in 1021 Japanese Parkinson's disease patients from 35 medical centers. *Parkinsonism Relat Disord* **38**, 54-60

56. Dunlop, B. W., and Nemeroff, C. B. (2007) The role of dopamine in the pathophysiology of depression. *Arch Gen Psychiatry* **64**, 327-337

57. Guillin, O., Abi-Dargham, A., and Laruelle, M. (2007) Neurobiology of dopamine in schizophrenia. *Int Rev Neurobiol* **78**, 1-39

58. Wojakiewicz, A., Januel, D., Braha, S., Prkachin, K., Danziger, N., and Bouhassira, D. (2013) Alteration of pain recognition in schizophrenia. *Eur J Pain* **17**, 1385-1392

59. Borsook, D., Linnman, C., Faria, V., Strassman, A. M., Becerra, L., and Elman, I. (2016) Reward deficiency and anti-reward in pain chronification. *Neurosci Biobehav Rev* **68**, 282-297

60. Ramdani, C., Carbonnell, L., Vidal, F., Béranger, C., Dagher, A., and Hasbroucq, T. (2015) Dopamine precursors depletion impairs impulse control in healthy volunteers. *Psychopharmacology (Berl)* **232**, 477-487

61. Baliki, M. N., Geha, P. Y., Fields, H. L., and Apkarian, A. V. (2010) Predicting value of pain and analgesia: nucleus accumbens response to noxious stimuli changes in the presence of chronic pain. *Neuron* **66**, 149-160

62. Martikainen, I. K., Nuechterlein, E. B., Peciña, M., Love, T. M., Cummiford, C. M., Green, C. R., Stohler, C. S., and Zubieta, J. K. (2015) Chronic Back Pain Is Associated with Alterations in Dopamine Neurotransmission in the Ventral Striatum. *J Neurosci* **35**, 9957-9965

63. Niikura, K., Narita, M., Butelman, E. R., Kreek, M. J., and Suzuki, T. (2010) Neuropathic and chronic pain stimuli downregulate central mu-opioid and dopaminergic transmission. *Trends Pharmacol Sci* **31**, 299-305

64. Leknes, S., and Tracey, I. (2008) A common neurobiology for pain and pleasure.

Nat Rev Neurosci **9**, 314-320

65. Rebouças, E. C., Segato, E. N., Kishi, R., Freitas, R. L., Savoldi, M., Morato, S., and Coimbra, N. C. (2005) Effect of the blockade of mu1-opioid and 5HT2A-serotonergic/alpha1-noradrenergic receptors on sweet-substance-induced analgesia. *Psychopharmacology (Berl)* **179**, 349-355
66. Roy, M., Peretz, I., and Rainville, P. (2008) Emotional valence contributes to music-induced analgesia. *Pain* **134**, 140-147
67. Becker, S., Gandhi, W., and Schweinhardt, P. (2012) Cerebral interactions of pain and reward and their relevance for chronic pain. *Neurosci Lett* **520**, 182-187
68. von Hehn, C. A., Baron, R., and Woolf, C. J. (2012) Deconstructing the neuropathic pain phenotype to reveal neural mechanisms. *Neuron* **73**, 638-652
69. Becker, S., Kleinböhl, D., and Hölzl, R. (2012) Awareness is awareness is awareness? Decomposing different aspects of awareness and their role in operant learning of pain sensitivity. *Conscious Cogn* **21**, 1073-1084
70. Schultz, W. (2007) Behavioral dopamine signals. *Trends Neurosci* **30**, 203-210
71. Lammel, S., Lim, B. K., Ran, C., Huang, K. W., Betley, M. J., Tye, K. M., Deisseroth, K., and Malenka, R. C. (2012) Input-specific control of reward and aversion in the ventral tegmental area. *Nature* **491**, 212-217
72. Fields, H. L. (1999) Pain: an unpleasant topic. *Pain* **Suppl 6**, S61-69
73. Navratilova, E., Xie, J. Y., Okun, A., Qu, C., Eyde, N., Ci, S., Ossipov, M. H., King, T., Fields, H. L., and Porreca, F. (2012) Pain relief produces negative reinforcement through activation of mesolimbic reward-valuation circuitry. *Proc Natl Acad Sci U S A* **109**, 20709-20713
74. Becker, S., Ceko, M., Louis-Foster, M., Elfassy, N. M., Leyton, M., Shir, Y., and Schweinhardt, P. (2013) Dopamine and pain sensitivity: neither sulpiride nor acute phenylalanine and tyrosine depletion have effects on thermal pain sensations in healthy volunteers. *PLoS One* **8**, e80766
75. Apkarian, A. V., Bushnell, M. C., Treede, R. D., and Zubieta, J. K. (2005) Human brain mechanisms of pain perception and regulation in health and disease. *Eur J Pain* **9**, 463-484

76. Kupfermann, I. (1991) Functional studies of cotransmission. *Physiol Rev* **71**, 683-732

77. Hu, S., Wang, J., Ji, E. H., Christison, T., Lopez, L., and Huang, Y. (2015) Targeted Metabolomic Analysis of Head and Neck Cancer Cells Using High Performance Ion Chromatography Coupled with a Q Exactive HF Mass Spectrometer. *Anal Chem* **87**, 6371-6379

78. Makarov, A., Denisov, E., Lange, O., and Horning, S. (2006) Dynamic range of mass accuracy in LTQ Orbitrap hybrid mass spectrometer. *J Am Soc Mass Spectrom* **17**, 977-982

79. Werner, E., Heilier, J. F., Ducruix, C., Ezan, E., Junot, C., and Tabet, J. C. (2008) Mass spectrometry for the identification of the discriminating signals from metabolomics: current status and future trends. *J Chromatogr B Analyt Technol Biomed Life Sci* **871**, 143-163

80. Miyazawa, H., Yamaguchi, Y., Sugiura, Y., Honda, K., Kondo, K., Matsuda, F., Yamamoto, T., Suematsu, M., and Miura, M. (2017) Rewiring of embryonic glucose metabolism via suppression of PFK-1 and aldolase during mouse chorioallantoic branching. *Development* **144**, 63-73

81. Miyajima, M., Zhang, B., Sugiura, Y., Sonomura, K., Guerrini, M. M., Tsutsui, Y., Maruya, M., Vogelzang, A., Chamoto, K., Honda, K., Hikida, T., Ito, S., Qin, H., Sanuki, R., Suzuki, K., Furukawa, T., Ishihama, Y., Matsuda, F., Suematsu, M., Honjo, T., and Fagarasan, S. (2017) Metabolic shift induced by systemic activation of T cells in PD-1-deficient mice perturbs brain monoamines and emotional behavior. *Nat Immunol*

82. Shariatgorji, M., Nilsson, A., Goodwin, R. J. A., Kallback, P., Schintu, N., Zhang, X. Q., Crossman, A. R., Bezard, E., Svenningsson, P., and Andren, P. E. (2014) Direct Targeted Quantitative Molecular Imaging of Neurotransmitters in Brain Tissue Sections. *Neuron* **84**, 697-707

83. Eisen, M. B., Spellman, P. T., Brown, P. O., and Botstein, D. (1998) Cluster analysis and display of genome-wide expression patterns. *Proc Natl Acad Sci U S A* **95**, 14863-14868

84. Altier, N., and Stewart, J. (1999) The role of dopamine in the nucleus accumbens in analgesia. *Life Sci* **65**, 2269-2287

85. Curatolo, A., D Arcangelo, P., Lino, A., and Brancati, A. (1965) Distribution of N-Acetyl-Asparatic and N-Acetyl-Aspartyl-Glutamic acids in nervous tissue. *J Neurochem* **12**, 339-342

86. Neale, J. H., Olszewski, R. T., Gehl, L. M., Wroblewska, B., and Bzdega, T. (2005) The neurotransmitter N-acetylaspartylglutamate in models of pain, ALS, diabetic neuropathy, CNS injury and schizophrenia. *Trends Pharmacol Sci* **26**, 477-484

87. Fukui, S., Matsuno, M., Inubushi, T., and Nosaka, S. (2006) N-Acetylaspartate concentrations in the thalami of neuropathic pain patients and healthy comparison subjects measured with (1)H-MRS. *Magn Reson Imaging* **24**, 75-79

88. Grachev, I. D., Fredrickson, B. E., and Apkarian, A. V. (2000) Abnormal brain chemistry in chronic back pain: an in vivo proton magnetic resonance spectroscopy study. *Pain* **89**, 7-18

89. Yamamoto, T., Kozikowski, A., Zhou, J., and Neale, J. H. (2008) Intracerebroventricular administration of N-acetylaspartylglutamate (NAAG) peptidase inhibitors is analgesic in inflammatory pain. *Mol Pain* **4**, 31

90. Yamada, T., Zuo, D., Yamamoto, T., Olszewski, R. T., Bzdega, T., Moffett, J. R., and Neale, J. H. (2012) NAAG peptidase inhibition in the periaqueductal gray and rostral ventromedial medulla reduces flinching in the formalin model of inflammation. *Mol Pain* **8**, 67

91. Nonaka, T., Yamada, T., Ishimura, T., Zuo, D., Moffett, J. R., Neale, J. H., and Yamamoto, T. (2017) A role for the locus coeruleus in the analgesic efficacy of N-acetylaspartylglutamate peptidase (GCPII) inhibitors ZJ43 and 2-PMPA. *Mol Pain* **13**, 1744806917697008

92. Miyamoto, Y., Ishikawa, Y., Iegaki, N., Sumi, K., Fu, K., Sato, K., Furukawa-Hibi, Y., Muramatsu, S., Nabeshima, T., Uno, K., and Nitta, A. (2014) Overexpression of Shati/Nat8l, an N-acetyltransferase, in the nucleus accumbens attenuates the response to methamphetamine via activation of group II mGluRs in mice. *Int J Neuropsychopharmacol* **17**, 1283-1294

93. Xi, Z. X., Li, X., Peng, X. Q., Li, J., Chun, L., Gardner, E. L., Thomas, A. G., Slusher, B. S., and Ashby, C. R. (2010) Inhibition of NAALADase by 2-PMPA attenuates cocaine-induced relapse in rats: a NAAG-mGluR2/3-mediated mechanism. *J Neurochem* **112**, 564-576